Critical Review on the Fate and Transport of Per- and Polyfluoroalkyl Substances (PFAS) in Subsurface Environments

Dengjun Wang[1], Xueyan Lyu[2], Feng Xiao[3], Chongyang Shen[4], Jingjing Chen[5], Chang Min Park[6], Yuanyuan Sun[7], and Markus Flury[8]

[1]Auburn University
[2]Nanjing University of Information Science and Technology
[3]University of North Dakota
[4]China Agricultural University
[5]Virginia Polytechnic Institute and State University
[6]Kyungpook National University
[7]Nanjing University
[8]Washington State University

November 22, 2022

Abstract

Per- and polyfluoroalkyl substances (PFAS), also known as "forever chemicals", are manmade chemicals that have been increasingly detected in various geological media since the early 2000s. The soil and subsurface environments are the geological media commonly affected by PFAS. We conducted a comprehensive review of peer-reviewed studies published from 2010 through 2021 concerning the fate and transport of PFAS in subsurface environments. This review is organized into different subsections, covering the basics of PFAS properties and how they affect the occurrence, fate, and transport of PFAS, the fundamental processes affecting subsurface transport and fate of PFAS, and mathematical models for describing and predicting PFAS transport behaviors. Mechanisms governing PFAS transport in the subsurface environment, including the sorption of PFAS at the air-water interface, solid-water interface, and nonaqueous phase liquids-water interface, were explored in detail. Challenges and future research priorities are identified to better combat the global challenges of PFAS contamination.

Hosted file

essoar.10508278.1.docx available at https://authorea.com/users/534400/articles/598470-critical-review-on-the-fate-and-transport-of-per-and-polyfluoroalkyl-substances-pfas-in-subsurface-environments

Critical Review on the Fate and Transport of Per- and Polyfluoroalkyl Substances (PFAS) in Subsurface Environments

Xueyan Lyu[1], Feng Xiao[2], Chongyang Shen[3], Jingjing Chen[4], Chang Min Park[5], Yuanyuan Sun[6], Markus Flury[7], and Dengjun Wang[8, *]

1. School of Hydrology and Water Resources, Nanjing University of Information Science and Technology, Nanjing 210044, China, Email: `xylyu@nuist.edu.cn`, ORCID: 0000-0003-3413-1466.

2. Department of Civil Engineering, University of North Dakota, Grand Forks, North Dakota 58202, USA, Email: `feng.xiao@und.edu`, ORCID: 0000-0001-5686-6055.

3. Department of Soil and Water Sciences, China Agricultural University, Beijing 100193, China, Email: `chongyang.shen@cau.edu`, ORCID: 0000-0002-2517-3472.

4. School of Plant and Environmental Sciences, Virginia Tech, Blacksburg, VA 24061, USA, Email: `jingji9@vt.edu`, ORCID: 0000-0002-5820-8360.

5. Department of Environmental Engineering, Kyungpook National University, 80 Daehak-ro, Buk-gu, Daegu 41566, Republic of Korea, Email: `cmpark@knu.ac.kr`, ORCID: 0000-0003-0541-0300.

6. Hydrosciences Department, School of Earth Sciences and Engineering, Nanjing University, Nanjing 210023, China, Email: `sunyy@nju.edu.cn`, ORCID: 0000-0002-4526-9287.

7. Department of Crop and Soil Sciences, Washington State University, Pullman and Puyallup, Washington 98371, USA, Email: `flury@wsu.edu`, ORCID: 0000-0002-3344-3962.

8. School of Fisheries, Aquaculture and Aquatic Sciences, Auburn University, Auburn, Alabama 36849, USA, Email: `dzw0065@auburn.edu`, ORCID: 0000-0002-2047-5260.

* Correspondence To:

Dengjun Wang

Email: `dzw0065@auburn.edu`

Phone: +(1) 334-844-9416

Graphic Abstract
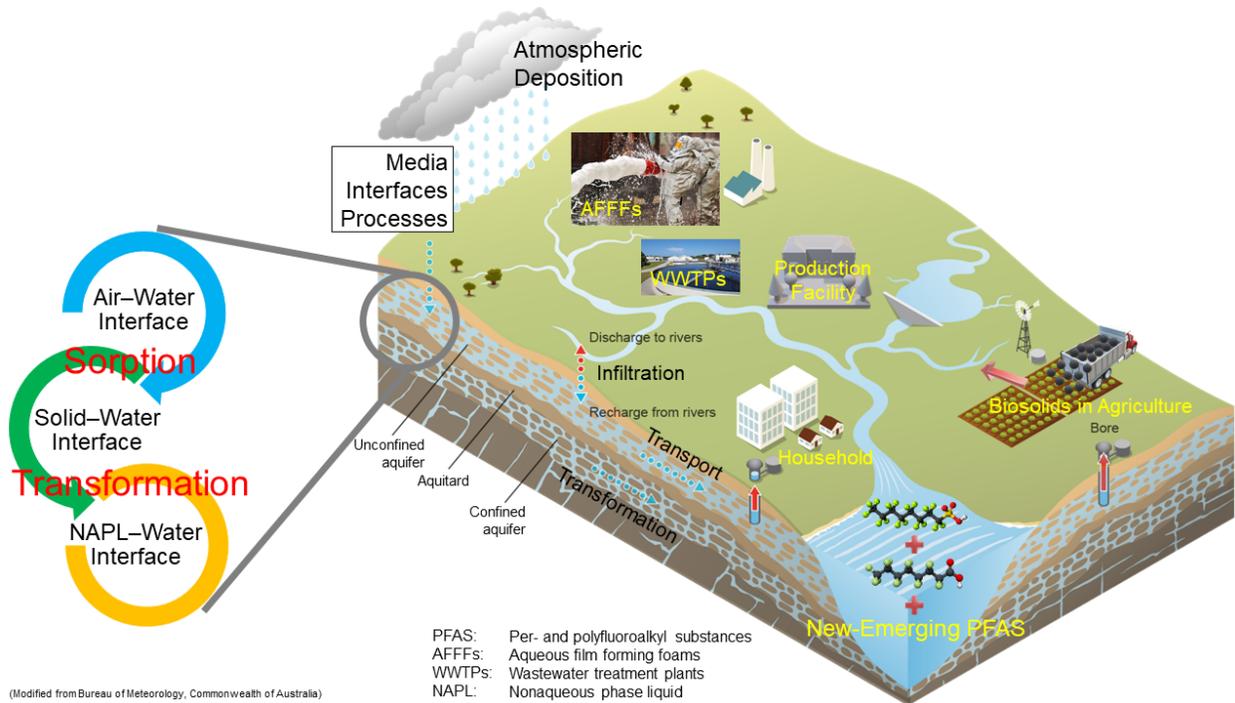
Key Words

Groundwater; Vadose Zone; Soil; Nonaqueous Phase Liquid (NAPL); Air–Water Interface; Solid–Water Interface; NAPL–Water Interface; Sorption; Retardation; Transport; Numerical Modeling; Contamination; Remediation

Key Points

- Key physicochemical properties of PFAS affecting their fate and transport in the subsurface are reviewed.

- Source, occurrence, and distribution of PFAS in various geological media are discussed.

- Mechanisms controlling PFAS sorption and retardation in the subsurface are illustrated.

- Effects of solid–water interface, air–water interface, and nonaqueous phase liquid on PFAS transport and retention are discussed in detail.

- Mathematical models governing PFAS transport and retention in subsurface porous media are summarized.

- Challenges and future research priorities and recommendation on PFAS monitoring, geological behaviors, risk assessment, management, and remediation are identified.

Glossary of Terms

AFFF Aqueous film forming foam

AWI Air–water interface

CMC Critical micelle concentration

FTSA Fluorotelomer sulfonate acid

GenX Ammonium salt of 2,3,3,3-tetrafluoro-2-(heptafluoropropoxy) propanoic acid

NAPLs Nonaqueous phase liquids

NWI NAPL–water interface

PFAAs Perfluoroalkyl acids

PFAS Per- and polyfluoroalkyl substances

PFBA Perfluorobutanoic acid

PFBS Perfluorobutane sulfonate acid

PFCAs Perfluoroalkyl carboxylic acids

PFHxA Perfluorohexanoic acid

PFHxS Perfluorohexane sulfonate acid

PFHpA Perfluoroheptanoic acid

PFHpS Perfluoroheptane sulfonic acid

PFNA Perfluorononanoic acid

PFOA Perfluorooctanoic acid

PFOAAmS Perfluoroctaneamido ammonium iodide

PFOS Perfluorooctanesulfonic acid

PFESAs Perfluoroether sulfonic acids

PFSAs Perfluoroalkyl sulfonic acids

SOC Soil organic carbon

SOM Soil organic matter

SWI Solid–water interface

WWTPs Wastewater treatment plants

K_a Acid dissociation constant

K_{ai} Partition coefficient at the air–water interface

K_d Solid–water partition coefficient

K_{ni} Partition coefficient at the NAPL–water interface

K_{OC} Organic carbon normalized distribution coefficient

K_{OW} Octanol–water partition coefficient

Abstract

Per- and polyfluoroalkyl substances (PFAS), also known as "forever chemicals", are manmade chemicals that have been increasingly detected in various geological media since the early 2000s. The soil and subsurface environments are the geological media commonly affected by PFAS. We conducted a comprehensive review of peer-reviewed studies published from 2010 through 2021 concerning the fate and transport of PFAS in subsurface environments. This review is organized into different subsections, covering the basics of PFAS properties and how they affect the occurrence, fate, and transport of PFAS, the fundamental processes affecting subsurface transport and fate of PFAS, and mathematical models for describing and predicting PFAS transport behaviors. Mechanisms governing PFAS transport in the subsurface environment, including the sorption of PFAS at the air water interface, solid water interface, and nonaqueous phase liquids water interface, were explored in detail. Challenges and future research priorities are identified to better combat the global challenges of PFAS contamination.

Plain Language Summary

PFAS are a group of manmade chemicals used in a multitude of applications and commercial products (clothing, cookware, cosmetics, personal care products, and fire extinguishers). Their widespread use has, however, lead to the release and distribution in terrestrial and aquatic ecosystems. PFAS, due to their unique properties, are very persistent in the environment as they do not degrade readily. Unfortunately, they are also toxic to organisms, including humans. In this review, we discuss the omnipresence of PFAS in water and soil and explain how PFAS move through subsurface media. There are thousands of different PFAS compounds, and only few of them have been studied in more detail and their transport behavior is known. PFAS tend to accumulate at the air–water interface in vadose zone. Generally, PFAS with long carbon chains are retained in soils more strongly than short-chain PFAS. Negatively charged PFAS are more mobile in soils than neutral and positively charged PFAS, and thus can readily pollute groundwater. Nonetheless, due to their persistence and slow desorption, even more strongly sorbed PFAS can be a sustained source for groundwater pollution. We finally identify challenges and future research needs to address the emerging threat of PFAS contamination of the environment.

1. **Introduction**

Per- and polyfluoroalkyl substances (PFAS; plural form) are a class of thousands of anthropogenic chemicals containing a fluorinated alkyl moiety of varying chain length (Figure 1) (Buck et al., 2011; ITRC, 2020; OECD, 2018). Due to their unique properties (e.g., hydro- and oleophobicity, and high chemical

and thermal stability), PFAS have been mass-produced and used for a wide array of industrial applications and commercial products since the 1940s (Buck et al., 2011; ITRC, 2020; OECD, 2018). These include textiles, packaging, household products, cosmetics, personal care products, paints, pesticides, and firefighting foams (e.g., aqueous film forming foams; AFFFs) (Buck et al., 2011; ITRC, 2020; OECD, 2018). In recent years, PFAS have garnered global attentions because of their persistence, bioaccumulation potential, and toxicity to wildlife and humans (Buck et al., 2011; ITRC, 2020; OECD, 2018). More than 3,000 PFAS compounds might have been manufactured (Wang et al., 2017), and the PFAS library is still growing very rapidly due to the improvement of analytical methods and instrumentation, including ultrahigh-performance liquid chromatography and high-resolution mass spectrometry.
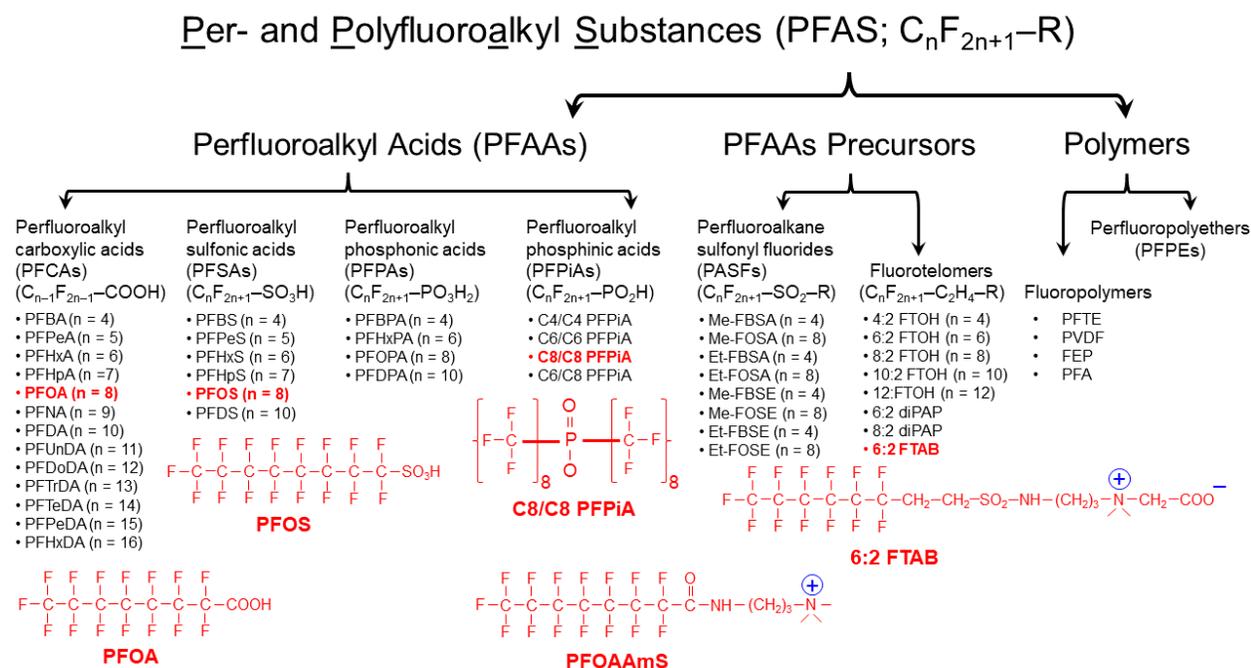
Figure 1. PFAS family tree including perfluoroalkyl acids (PFAAs), PFAAs precursors (e.g., perfluoroalkane sulfonyl fluorides and fluorotelomers), and polymers (e.g., fluoropolymers and perfluoropolyethers). PFAAs include perfluoroalkyl carboxylic acids (PFCAs), perfluoroalkyl sulfonic acids (PFSAs), perfluoroalkyl phosphonic acids (PFPAs), perfluoroalkyl phosphinic acids (PFPiAs), perfluoroether carboxylic acids (PFECAs), and perfluoroether sulfonic acids (PFESAs). Molecular structures of typical PFAS compounds (in red) including anionic PFOA and PFOS, C8/C8 PFPiA, cationic perfluoroctaneamido ammonium iodide (PFOAAmS), and zwitterionic 6:2 fluorotelomer sulfonamide alkylbetaine (FTAB) are highlighted.

Recently, PFAS have been increasingly detected in wildlife, including invertebrates, fish, amphibians, reptiles, birds, and mammals worldwide (Ahrens, 2011; De Silva et al., 2021; Giesy and Kannan, 2001). Also, humans are exposed to PFAS through a wide variety of pathways such as dietary ingestion, drinking water ingestion, personal care products and cosmetics exposure, dust inhalation, and indoor air exposure (De Silva et al., 2021; Morales-McDevitt et al., 2021; Sunderland et al., 2019). Multiple lines of evidence have shown the links between PFAS exposure and adverse human health effects, such as endocrine disruption, hepatic, reproductive, and developmental toxicity, kidney and testicular cancer, neurotoxicity, immunotoxicity, and genotoxicity, particularly for pregnant women, fetuses, and children (Figure 2) (ATSDR, 2021; C8 Science Panel, 2012; IARC, 2017). To mitigate potential adverse effects, the U.S. Environmental Protection Agency has issued a health advisory level for two primary PFAS compounds, i.e., perfluorooctanoic acid (PFOA) and perfluorooctanesulfonic acid (PFOS) (Figure 1) in drinking water at 70 ng/L in 2016 (USEPA, 2016a; b). Certain U.S. states have begun to promulgate even more stringent limits for PFOA, PFOS, and other PFAS, attempting to minimize the potential adverse impacts of PFAS to human health, wildlife, and the environment (Post, 2021). These include perfluorobutanoic acid (PFBA), perfluorobutane sulfonate acid (PFBS), perfluorohexanoic acid (PFHxA), perfluorohexane sulfonate acid (PFHxS), and perfluoroheptanoic acid (PFHpA) (Figure 1) (Post, 2021).

PFAS Human Health Effect

Developmental Effects Affecting Unborn Baby
- **Delayed mammary gland development**
- **Reduced response to vaccines**
- **Lower birth weight**
- Obesity
- Early puberty onset
- Increased miscarriage risk (pregnancy loss)
- Lower sperm count and mobility

- Thyroid disease
- Increased cholesterol levels
- Breast cancer
- **Liver damage**
- **Kidney cancer**
- Inflammatory bowel disease
- **Testicular cancer**
- Increase time to pregnancy
- Pregnancy induced hypertension (increased blood pressure)

—— **High certainty**
········· Low certainty

Figure 2. Effects of PFAS on human health. PFAS exposure is linked to

thyroid disease, increased cholesterol level, liver damage, kidney cancer, and testicular cancer, particularly for pregnant women, fetuses, and children (e.g., delayed mammary gland development, reduced response to vaccines, and lower birth weight). Sources: U.S. National Toxicology Program (ATSDR, 2021), C8 Science Panel (2012), IARC Working Group on the Evaluation of Carcinogenic Risks to Humans (2017), Barry et al. (2013), Fenton et al. (2009), and White et al. (2011). European Environment Agency, 2021, "Effects of PFAS on human health (https://www.eea.europa.eu/signals/signals-2020/infographics/effects-of-pfas-on-human-health/view) accessed on 10/05/2021". Copyright: European Environment Agency (reproduction with permission).

Understanding the fate and transport of PFAS in different geological media is needed to evaluate their potential risks and develop effective strategies for managing and remediating contaminated sites. The soil and subsurface environments are the geological media commonly affected by PFAS, primarily because of the disposal of PFAS-containing waste materials, application of PFAS-containing biosolids, and the use of PFAS-based film-forming forms for fire-training and fire suppression activities. The number of studies investigating the fate and transport of PFAS in subsurface environments, as well as the effects of PFAS properties and geological factors (e.g., soil and water chemistry) on these transport processes has increased considerably in recent years. To facilitate the identification of general PFAS transport patterns, reviews have been complied on how geological factors particularly including environmental parameters affect the transport and retention of PFAS in subsurface environments. For example, Sharifan et al. (2021) recently performed a systematic review on the source, distribution, and speciation of PFAS in the vadose zone and how the physico-chemical processes affect the sorption, biotransformation, and plant uptake of PFAS in soil. Borthakur et al. (2021) reviewed the roles of suspended particles on the distribution of PFAS in surface runoff, surface water, and subsurface soil. Sima and Jaffe (2021) discussed the sorption mechanisms (isotherms and kinetics) of PFAS in soil. These reviews have provided important insights into advancing our understandings of the mechanisms controlling PFAS transport in surface and subsurface environments. However, these reviews have mostly focused on legacy PFAS (e.g., anionic PFOA and PFOS; Figure 1). Recently, numerous cationic and zwitterionic PFAS compounds have been identified (e.g., cationic perfluoroctaneamido ammonium iodide (PFOAAmS), and zwitterionic 6:2 fluorotelomer sulfonamide alkylbetaine (FTAB); Figure 1) (Barzen-Hanson et al., 2017b; Xiao, 2017). Furthermore, a few PFOA and PFOS alternative compounds have been identified in the environmental and drinking water samples (Heydebreck et al., 2015; Sun et al., 2016), which may pose a potential risk to the human health. Additionally, recent studies have demonstrated that PFAS transport can be retarded in the vadose zone due to the adsorption on air (e.g., at the air–water interface; AWI) (Brusseau, 2018; Brusseau et al., 2019; 2021). However, our knowledge on the fate and transport of these novel PFAS compounds in subsurface environments (e.g., in the vadose zone rich in AWIs) remains limited.

In this critical review, we provide a state-of-the-art synthesis of the scientific advancement on how the properties of PFAS, in concert with geological factors (soil and water chemistry) influence the sorption, retardation, and transport of both conventional (e.g., anionic) and novel (e.g., cationic and zwitterionic) PFAS in subsurface environments (Figure 3). We performed a systematic literature search on Web of Science (https://www.webofscience.com/), Scopus (https://www.scopus.com/), and Google Scholar (https://scholar.google.com/). Inclusion criteria were original studies or review articles on the fate and transport of PFAS published in English-language journals between 2010 and 2021. We surveyed the environmental concentrations of PFAS in soil, surface water, sea, ocean, and groundwater to demonstrate that their transport potential is strongly impacted by their perfluorinated carbon chain length, functionality, and polarity (Figure 1). Moreover, we evaluated how nonaqueous phase liquids (NAPLs) affect the mobility and retardation of PFAS in the subsurface. We then summarized the mathematical models that can describe and predict the transport of PFAS in unsaturated and saturated zones. We conclude our review by identifying key challenges and future research priorities for PFAS monitoring and identification, geological behavior, risk assessment, and contaminated site management and remediation to combat the vexing PFAS contamination.
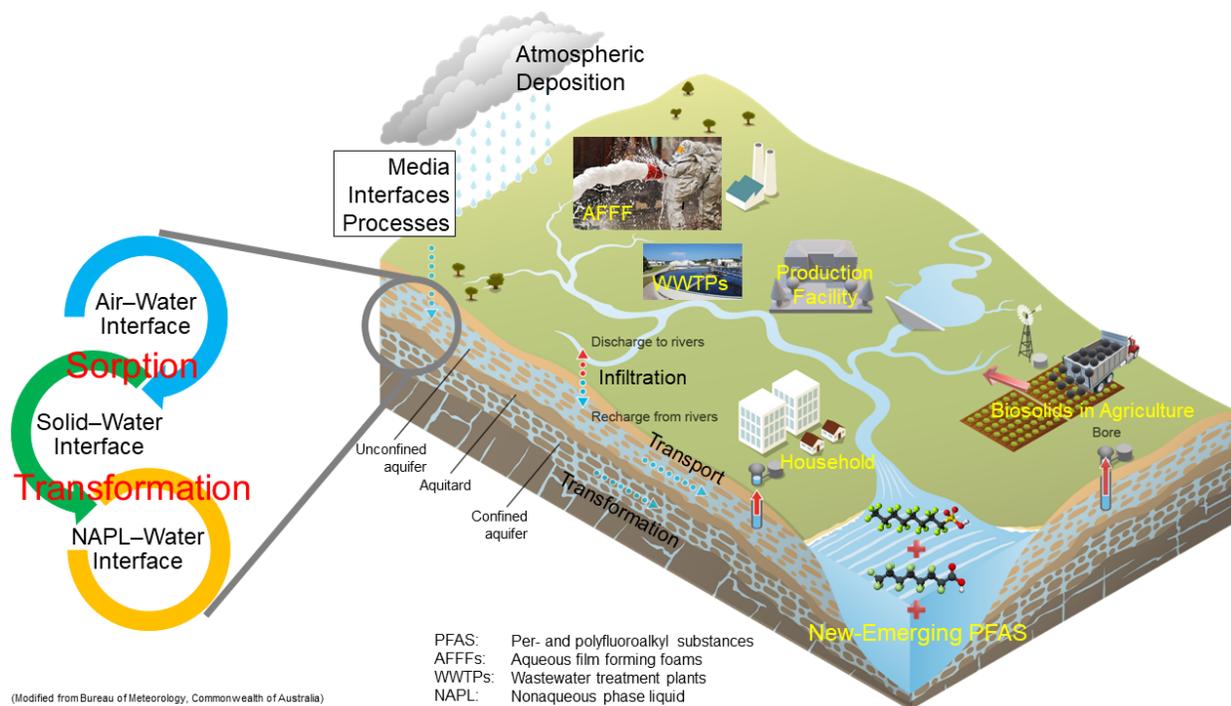
Figure 3. Major contamination sources (e.g., AFFFs, WWTPs, PFAS production facility, household release, and biosolid use in agriculture), and processes affecting the fate and transport of PFAS in different geological media (e.g., atmo-

sphere, soil, surface water, and groundwater). Key interfaces such as air–water interface (AWI) in the vadose zone, solid–water interface (SWI), and NAPL–water interface (NWI) affecting PFAS transport and retention are highlighted.

1. PFAS Classification and Physicochemical Properties

(a) PFAS Classification

The U.S. Environmental Protection Agency categorizes PFAS into long-chain (8C) and short-chain (7C) PFAS, based upon the total carbon number in PFAS molecules (USEPA, 2009). PFAS family can be further categorized as perfluoroalkyl acids (PFAAs), polyfluoroalkyl substances, and polymers including fluoropolymers and perfluoropolyethers (PFPEs) (Figure 1) (Wang et al., 2017). Perfluoroalkyl carboxylic acids (PFCAs, e.g., PFOA) and perfluoroalkyl sulfonic acids (PFSAs, e.g., PFOS) are two most important classes of PFAAs, which have received significant scientific and regulatory attention. This is largely due to the widespread use (e.g., PFOS in AFFF formulations; Figure 3) (SERDP-ESTCP, 2017) and higher concentrations of PFAAs in the environment compared to other PFAS compounds. In contrast, perfluoroalkyl phosphinic acids (PFPiAs), and perfluoroether carboxylic and sulfonic acids (PFECAs and PFESAs) have been largely underexplored by the scientific community. PFOA and PFOS have phased out of production since 2015 in the U.S., but they are still ubiquitously abundant in the environment, including surface water and groundwater (Anderson et al., 2019; Brusseau and Van Glubt, 2019; Hatton et al., 2018). Furthermore, various studies have documented that PFAAs, including PFOS and PFOA, can be generated from precursor compounds in chemical (Xiao et al., 2018; Zhu et al., 2019), biological (Lenka et al., 2021; Mejia-Avendano et al., 2016; Xiao et al., 2018), and thermal processes (Sasi et al., 2021; Xiao et al., 2020; 2021).

Short-chain PFAS such as C4 PFBA and PFBS have been widely manufactured to replace the long-chain PFAS. While a consensus has been reached on that shorter-chain PFAS have less potential for bioaccumulation and higher mobility in the environment, little research is available on their environmental impacts and potential human health risks (Brendel et al., 2018; Li et al., 2020). Especially, shorter-chain PFAS are more recalcitrant against transformation and degradation in certain systems due to the stronger carbon–fluorine (C–F) bonds with greater persistence and lifespan in the environment (ITRC, 2020).

1. PFAS Physicochemical Properties

PFAS are usually in a solid physical state at room temperature but can be dissolved in water to a limited degree. Several short-chain PFAS (e.g., C4 PFBA and PFBS) are shown in a liquid phase at room temperature and easier to be dissolved in the water (Williams et al., 2017). Generally, PFAS with longer carbon chain have lower water solubility. However, data on solubilities are rare. PFOS and PFOA, two of the more studied PFAS compounds, have water solubilities of 550–570 and 9,500 mg/L, respectively, at 25 °C (USEPA, 2014). PFAS are chemically and thermally stable under room environment. However,

some PFAS compounds may be light sensitive (e.g., PFBS), and can interact with air (e.g., PFBA and PFBS) and need to be stored in cool conditions (e.g., PFBA). PFAS may show a strong acidity (low acid dissolution constant; pK_a) when they are paired with an acid functional group.

Many PFAS are surfactants with a special molecular structure: consisting of a hydrophobic fluoroalkyl chain (repellent to the liquid for both oil and water) with hydrophilic functional group (attracted to aqueous liquids) at one end (Figure 1). With this unique molecular structure, PFAS exhibit surfactant-related properties that determine their fate, sorption, and transport in the natural environment. Like a typical hydrocarbon-based surfactant, low concentration of PFAS can mix with a polar liquid to reduce its surface tension. Unlike hydrocarbon-based surfactants, however, the perfluorinated chain of PFAS is both hydrophobic (water repellent) and oleophobic (oil and fat repellent) (Xu et al., 2017), while the polar functional moiety is hydrophilic. This unique attribute suggests that PFAS compounds tend to concentrate at the interfaces. The stable molecular structure of PFAS also explains their high resistance to environmental transformation, including biodegradation, photooxidation, direct photooxidation, direct photolysis, and hydrolysis (Buck et al., 2011; ITRC, 2020).

The hydrophobic and oleophobic properties limit their concentration in the soil pore water, which causes strong accumulation of PFAS at the air–water interface (AWI) in the vadose zone (Anderson et al., 2019; Brusseau et al., 2021). In general, the surface tension of soil solution decreases with increasing PFAS concentration. Current research efforts have focused largely on individual PFAS, and rarely considered PFAS mixtures, although the PFAS at contaminated sites are known to occur as complicated PFAS mixtures (Anderson et al., 2016; McGregor and Zhao, 2021). Only a few studies have reported the surface tensions of PFAS mixtures (Figure 4), and generally the compound with the lowest surface tension controls the overall surface tension/activity of the mixtures (Brusseau and Van Glubt, 2019; Vecitis et al., 2008). For example, Vecitis et al. (2008) reported that the surface tension curve of PFOA–PFOS binary mixture overlaps with that of PFOS since surface tension of PFOS is lower than PFOA (Figure 4c). Silva et al. (2021) conducted similar surface tension measurements for PFCA mixtures, and reported that competitive adsorption between PFAS compounds occurs at the AWI, in which the adsorption is controlled by the compound with greater surface activity (Figure 4b). An exception was documented by Schaefer et al. (2019) with mixtures of PFOS and fluorotelomer thioether amido sulfonate, i.e., the mixtures exhibited intermediate effects on surface tensions as compared to the individual compounds. These findings suggest that the interfacial sorption of mixed PFAS is not impacted by each other. The relationship between the surface tension of mixtures and their concentrations is not always consistent. For instance, the aqueous solution of oppositely charged surfactant mixture shows a more surface-active character (lower surface tension) compared to that of individual surfactants, due to the formation of an ionic complex between oppositely charged surfactants (Tajima et al., 1979). There-

fore, more studies are needed to investigate the surface tension properties of PFAS mixture, particularly including novel different charged PFAS compounds (Figure 1).
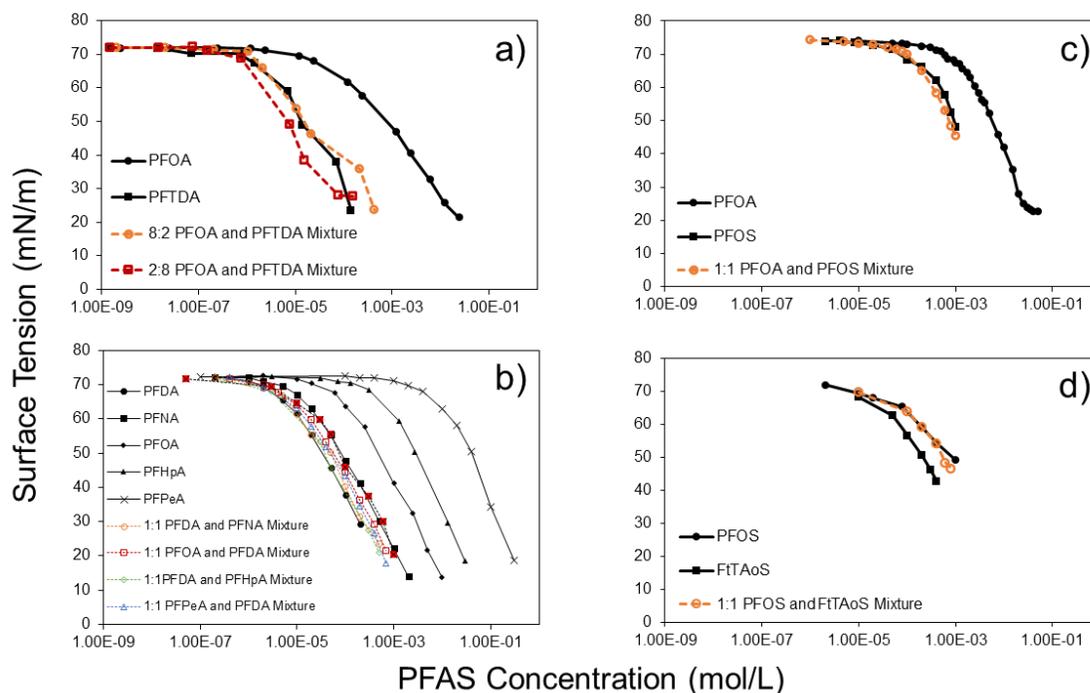

Figure 4. Surface tension of individual PFAS compounds and PFAS mixtures as a function of concentration. Data for panels (a–d) were extracted from Brusseau and Glubt (2019), Silva et al. (2021), Vecitis et al. (2008), and Schaefer et al. (2019), respectively. Copyrights: 2019 Elsevier (a), 2021 Elsevier (b), 2008 American Chemical Society (c), and 2019 American Chemical Society (d) (reproduction with permission).

The critical micelle concentration (CMC) is an important characteristic of surfactants, because at this concentration the chemicals will aggregate and form colloidal (micelle) suspensions in solution, thereby changing the overall surface properties and the sorption and transport behavior in geologic media. The CMC of PFAS depends on their surface tension. Long-chain PFAS (e.g., PFOA) can form hemi-micelle when their concentrations range between 0.01–0.03-folds of their CMCs (Xiao et al., 2011; Xu et al., 2020). The surface activity of surfactant mixtures could be complex, depending on the interactions between different surfactants. Research on the surface activity of fluorocarbon surfactant mixtures is seldom, but we can get some insights from studies on fluorocarbon-hydrocarbon surfactant mixtures and hydrocarbon-hydrocarbon surfactant mixtures. For example, adding dissimilarly charged hydrocarbon surfactants to anionic fluorocarbon surfactants is observed to decrease the CMC of PFAS by 60%, 75%,

and 30-folds, when adding nonionic surfactant, zwitterionic hydrocarbon surfactant, and cationic hydrocarbon surfactants, respectively (Brusseau and Van Glubt, 2019). In contrast, the CMC of mixed similarly charged fluorocarbon-hydrocarbon surfactant increases due to the antagonistic behavior from repulsive interaction between two different hydrophobic groups. Thus far, only one relevant study reported the CMC of fluorocarbon-fluorocarbon surfactant mixture (Yoda et al., 1989). Mixing two surfactants with similar hydrophobic groups, including hydrocarbon-hydrocarbon and fluorocarbon-fluorocarbon mixtures, showed a good mixing behavior. Specifically, the CMC of the mixtures ranges between the highest to the lowest CMCs of the individual surfactants. Furthermore, the CMC of mixtures generally varies as a smooth monotonic function, depending on the mass fraction of individual surfactants in the mixtures (Yoda et al., 1989). Most reported CMCs of individual PFAS compounds are much higher than the concentrations observed in groundwater, even considering the fact that the CMCs of PFAS vary with environmental conditions (e.g., pH, ionic strength and composition, and co-contaminants) (Bhhatarai and Gramatica, 2011; Brusseau, 2018; Fang et al., 2019). Therefore, the surface tension of PFAS mixtures at concentrations below CMCs is more practically important, particularly with regard to understanding their fate and transport in different geological settings such as vadose zone and groundwater.

1. **PFAS Source, Occurrence, and Distribution**

Understanding the source, occurrence, and distribution of PFAS in subsurface environments is a prerequisite for assessing the contamination status, managing exposure risk, and developing effective management and remediation strategies for contaminated sites. While PFAAs, including PFOA and PFOS, are perhaps the most commonly monitored and reported PFAS in the environment on a global scale (Muir and Miaz, 2021; Podder et al., 2021), many other classes of PFAS, such as GenX (the ammonium salt of 2,3,3,3-tetrafluoro-2-(heptafluoropropoxy) propanoic acid) and polyfluoroalkyl substances, have recently been increasingly detected in various geological media (e.g., soil, surface water, river, sea, ocean, and groundwater) (Xiao, 2017). PFAS can result from manufacturing and use of these chemicals and related products, as well as from the transformation of precursor compounds in environmental and engineered systems (Mejia-Avendano et al., 2016; Xiao et al., 2012; 2018). PFAS can be released to the aquatic environment through direct and indirect pathways (Figure 3). Direct pathways include atmospheric deposition (Scott et al., 2006; Simcik and Dorweiler, 2005), AFFF use in airports and military fire-training areas, and accidental release (Moody et al., 2002). Land applications of biosolids and municipal sludge from wastewater treatment plants (WWTPs) (Hamid et al., 2018), and irrigation with PFAS-containing waters are regarded as indirect sources of PFAS (Figure 3).

1. **Atmospheric Deposition**

Atmospheric deposition is recognized as one of the major contributors of PFAS dissemination to aquatic and terrestrial environments (Figure 3), particularly in

remote (Arctic and Antarctic regions) and rural areas with fewer anthropogenic sources nearby (Giesy and Kannan, 2001). PFAS present in air can be in the gaseous form or be bound to particulates due to industrial stack emissions or through fugitive emissions from manufacturers, storages, and transport in supply and waste streams (Dreyer et al., 2010). Neutral volatile polyfluorinated precursors such as fluorotelomer alcohols (FTOHs; Figure 1) are reported as the dominant polyfluorinated compounds in indoor air (Morales-McDevitt et al., 2021; Schlummer et al., 2013), where ~60% of detected PFAS are bound to particulates. This triggers great concerns on human exposure to these neutral volatile PFAS, since humans typically spend ~90% of their time indoors (Morales-McDevitt et al., 2021). In addition to neutral volatile polyfluorinated precursors, gaseous and particle bound PFAS may be ionic species, such as legacy PFOA and PFOS and new PFAS alternatives (e.g., perfluoroalkyl ether carboxylic acids and GenX) (D'Ambro et al., 2021; Shimizu et al., 2021). A few studies have revealed wind as an important vector of airborne PFAS (Barton et al., 2010; Schroeder et al., 2021; Xiao et al., 2015). For instance, Xiao et al. (2015) found that the levels of PFOA and PFOS in soil decrease more rapidly in the upwind direction than in the downwind direction from a point source of contamination. This suggests wind as a potential pathway for off-site transport of airborne particle-bond PFAS. The atmospheric lifetime of certain polyfluorinated species is several days (Sharifan et al., 2021), which can undergo atmospheric oxidation to form other species, including PFAAs, before eventually reaching to the Earth's surface via wet or dry deposition (Shimizu et al., 2021). Atmospheric deposition can cause widespread dissemination of PFAS to soil, but the maximum PFAS soil contamination generally occurs within tens to hundreds of km from the sources (e.g., fluorochemical manufacturers), as predicted by Gaussian diffusion models (D'Ambro et al., 2021; Shimizu et al., 2021; Zhou et al., 2021).

1.   Use and Application of PFAS-Containing AFFFs

Aqueous film forming form (AFFF) formulations have been used to extinguish hydrocarbon fuel fires since the 1960s (Anderson et al., 2016; SERDP-ESTCP, 2017; USGAO, 2018). The military sector is estimated to consume 75% of the AFFFs on the market, with the remaining (25%) being used by municipal airports, refineries, fuel tank farms, and other industries in the U.S. (Darwin, 2011). AFFF formulations are highly effective in suppressing fires, and they work by coating the burning material with a foam, thereby cutting off the supply of oxygen (SERDP-ESTCP, 2017). AFFF formulations are a complex proprietary mixture of chemicals with various hydrocarbon- and fluorine-containing surfactants that include 1–4% (w/w) PFAS (ITRC, 2020; Luo et al., 2020). AFFF formulation is typically diluted to a 3–6% (v/v) as a solution concentrate for use in fire suppression (Leeson et al., 2021; Silva et al., 2019). Hundreds of PFAS species have been identified in AFFF formulations with a significant amount of PFOS, PFHxS, and other PFSAs and PFCAs (Field et al., 2017). For instance, the AFFF formulations manufactured by 3M in 1993 include 78% PFSAs and 3% PFCAs (Field et al., 2017). These belong to legacy AFFFs produced mainly

by electrochemical fluorination process (Buck et al., 2011). After the voluntary phaseout of PFOS and its precursors around 2000, manufacturers start to produce AFFFs heavily through the fluorotelomerization process, which generates fluorotelomer alcohols (6: 2 and 8: 2 FTOH; Figure 1) (Backe et al., 2013; Buck et al., 2011). The use of both legacy (via electrochemical fluorination) and contemporary (via fluorotelomerization) AFFFs has caused PFAS contamination in adjacent surface water, groundwater, soil, sediment, and biota (Leeson et al., 2021; Ruyle et al., 2021a). PFOS is still the major species in AFFFs-impacted sites due to historical mass production and application. Nonetheless, recent findings based on nontargeted high resolution mass spectrometry analyses show that fluorotelomers (e.g., n: 2; n = 4, 6, and 8; Figure 1) account for 90% of PFAS mass in contemporary AFFF products (Ruyle et al., 2021b). Houtz et al. (2013) found that precursor compounds of PFAAs accounted for 41 100%, 23%, and 28% of the total concentration of PFAS in AFFF samples, groundwater, and solid samples, respectively. Houtz et al. (2013) believed that much of the mass of precursor compounds originally present in AFFF was converted to PFAAs once released to soil and groundwater. More than 400 sites have been identified in the U.S. where known or suspected release of PFAS to soil has occurred due to the use of AFFFs for fire training (DOD, 2017). It is imperative to obtain a more comprehensive understanding of PFAS transport in AFFF-impacted areas to facilitate the development of appropriate management and remediation strategies.

In addition to anionic PFOS and fluorotelomers, cationic and zwitterionic PFAS (Figure 1) have been increasingly detected in AFFFs and AFFFs-contaminated soil and water samples (Backe et al., 2013; D'Agostino and Mabury, 2017; Nickerson et al., 2021; Xiao et al., 2017). Cationic and zwitterionic PFAS accounted for ~50% of newly identified PFAS compounds (Xiao, 2017), and have been found to compose up to 97% of the total PFAS mass in soils of a fire-training area (Nickerson et al., 2021). D'Agostino and Mabury (2017) reported that a few of cationic and zwitterionic PFAS compounds were widespread in Canadian surface waters. Many of these compounds are structurally similar to PFAAs, except that the perfluoroalkyl chain is attached to a non-fluorinated moiety that may degrade to form PFAAs (thereafter referred to as precursor compounds of PFAAs). For example, certain cationic and zwitterionic PFAS can convert to PFAAs (e.g., PFOA and PFOS) through oxidation pathways (Xiao et al., 2018) or biotransformation in terrestrial invertebrates (Jin et al., 2020). Nickerson et al. (2021) performed a comprehensive study on PFAS in both soil (N = 105) and groundwater (N = 58) samples collected from an AFFF-impacted site. The authors found that PFAS concentrations were usually higher at depth than near the surface in soil (Nickerson et al., 2021), which is consistent with the previous findings reported by Xiao et al. (2015). In particular, the percentage of branched PFOS increased with depth, which agrees with the sorption capacities of linear and branched PFOS isomers to soil (Xiao et al., 2015). On the other hand, the *in situ* transformation of fluorotelomer compounds can cause an enrichment of linear PFOA (Xiao et al., 2015). Similarly, Adamson et al.

(2020) observed that PFAAs and their precursor compounds accounted for 48% and 52%, respectively, of the total PFAS mass measured in AFFF-impacted sites. Zwitterionic and cationic PFAS were primarily reported in the source and up/side-gradient areas, representing 83% of the total precursor mass. The authors also estimated that the conversion rate of precursor compounds to PFAAs was >2% annually. These findings suggest a low mobility of cationic and zwitterionic PFAS chemicals, likely due to the strong adsorption by soil (Xiao et al., 2019). Nonetheless, more research is still needed to better unravel the composition of AFFF-contaminated geological media, particularly for the novel PFAS and their transformation products in the environment.

1. **Reclaimed Wastewater for Irrigation and Biosolids**

Besides AFFFs use, municipal and industrial waste disposal sites, WWTPs, landfills, and biosolids are also major sources of PFAS contamination (Figure 3). Wastewater acts as a significant determinant of PFAS pollution in urban watersheds. In the U.S., there are currently no regulatory limits for PFAS in industrial wastewater, meaning that chemical plants do not have to control the release of PFAS in their wastewater; however, legislation to establish such limits is underway [Hogue, 2021]. Conventional wastewater and sludge treatment systems have been reported to be ineffective in removing PFAS (Arvaniti and Stasinakis, 2015). For example, Xiao et al. (2012) reported concentrations of PFAAs in the influent and effluent from 37 WWTPs and concluded that conventional and advanced and/or tertiary wastewater treatment (e.g., UV sterilization) did not significantly remove PFAS from wastewater. Instead, concentrations of studied PFAAs, including PFOA and PFOS, increased after biological wastewater treatment in certain surveyed WWTPs (Xiao et al., 2012). These findings indicate the de novo formation of PFAAs, which is likely due to the biodegradation of precursor compounds in WWTPs (Xiao et al., 2012).

In the U.S., the PFAS content in biosolids is estimated to be 500–6,000 µg/kg (Ghisi et al., 2019), depending upon the nature of treatment processes from where PFAS are released, as well as the treatment processes (e.g., blending, heat treatment, composting, and thermal hydrolysis) in WWTPs (USEPA, 2018). Previous studies have shown that applying both industrially contaminated and typical municipal biosolids as a soil amendment can transfer PFAAs to the soil, with higher application frequency resulting in increased PFAAs concentration (Sepulvado et al., 2011). Preferential leaching of short-chain PFCAs (C7) was observed in biosolids-amended soil cores at depths of 1.2 m or more (Sepulvado et al., 2011; Washington et al., 2010). Among the four treatment processes of biosolids, only the biosolids blended with PFAS-free materials are expected to have a lower PFAAs concentration due to the dilution effect (Lazcano et al., 2019). Heating and composting treatments likely increase PFAAs concentration due to transformation of polyfluorinated precursors to PFAAs (Bolan et al., 2021; Sharifan et al., 2021). Therefore, the PFAAs level in biosolids is increased after wastewater treatment (Lenka et al., 2021). In addition, part of the PFAAs precursors remained in biosolids may transform to more persistent PFAAs after

land application due to biotransformation (Bolan et al., 2021; Sharifan et al., 2021).

The annual loading of PFAS in the U.S. biosolids is estimated to range 2,749–3,450 kg/year, among which 1,375–2,070 kg/year of PFAS in biosolids is applied to agricultural lands and 467–587 kg/year to landfills, respectively (Venkatesan and Halden, 2013). PFOS is monitored as the most abundant compounds in biosolids with a mean concentration of 403 ± 127 ng/g, followed by PFOA (34 ± 22 ng/g), perfluorodecanoic acid (26 ± 20 ng/g), and others (e.g., PFHxA, PFBA, PFBS, PFHxS, and perfluoropentanoic acid) (Lakshminarasimman et al., 2021; Lenka et al., 2021; Venkatesan and Halden, 2013). These results are consistent with the data reported by Higgins et al. (2005) that total PFAS concentrations in domestic sludges vary between 55 and 3,370 ng/g, in the U.S. Similar magnitudes of PFAS contents in biosolids are reported in other countries such as in Nordic countries (0.6–15.2 ng/g) (Kallenborn, 2004), China (9.2–307 ng/g) (Wang et al., 2015), Switzerland (28–637 ng/g) (Sun et al., 2011), and Australia (4.2–910 ng/g) (Moodie et al., 2021).

1. **PFAS Concentrations in Water and Soil**

    (a)   PFAS Concentrations in Water (Surface Waters, Seawaters, Oceans, and Groundwater)

Since the early 2000s, PFAS compounds have been widely detected in global surface waters. A meta-analysis of PFAS concentrations in global surface waters, including rivers, lakes, tributaries, estuaries, canals, reservoirs, drainage basins, and creeks was recently reported by Podder et al. (2021). Figure 5 shows the global occurrence of PFOA and PFOS in surface waters during the past two decades (2001–2010 and 2011–2020). Apparently, PFOA and PFOS occurred in almost all collected water samples, and PFOS had a higher concentration than PFOA. For example, median concentrations of PFOS and PFOA in Asian surface waters between 2001–2010 reached 2,715 and 167 ng/L, respectively (Podder et al., 2021). A 10-fold higher concentration of both PFOS and PFOA was observed in surface waters in China, Australia, and Europe, compared to that in North and South America. Still, high concentrations of PFOS and PFOA (e.g., 5–10 folds higher than the health advisory limit of 70 ng/L issued by the U.S. Environmental Protection Agency) occurred in surface waters in 2001–2010 (Figure 5). These findings suggest that phasing out of PFOS and its precursors by 3M around 2000 did not have an immediate impact on the reduction of PFOS concentrations between 2000–2010, and a decrease in PFOS concentration started to occur since 2011. In addition to PFOS and PFOA, other PFAS compounds, particularly including PFHpA, PFHxA, PFNA, and PFBS, were widely detected in global surface waters. For instance, the short-chain PFBS concentration increased significantly after 2010 in Asian countries (e.g., China and Japan) (Podder et al., 2021). This again correlates with the substitution of long-chain PFAS by short-chain PFAS in response to the changes of PFAS use regulations, as discussed above. While anionic PFAS dominate the overall mass and concentration of PFAS detected in global groundwater,

zwitterionic and cationic PFAS also play a role (Hatton et al., 2018). Overall, globally high PFAS concentrations have been observed in Asia (China, Japan, Korea, and Australia) and Europe (Germany, U.K., and the Netherlands). This is partly because China is one of the largest producers and consumers of PFAS globally (Li et al., 2015).
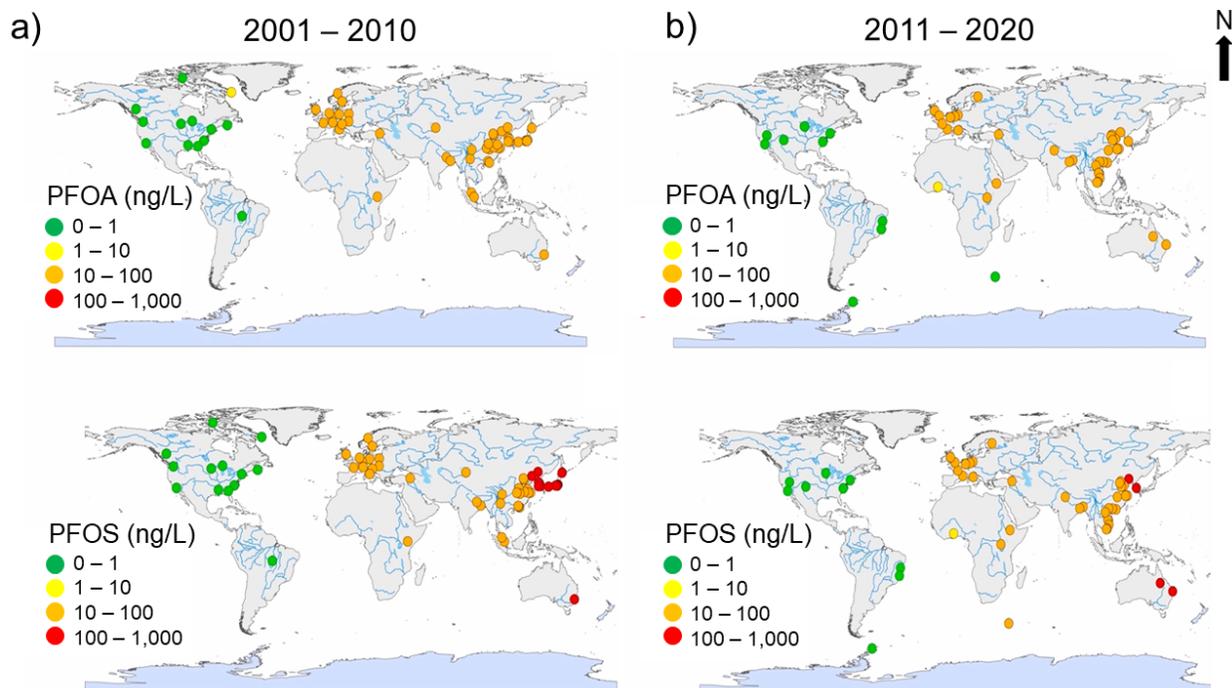

Figure 5. Global concentrations (ng/L) of perfluorooctanesulfonic acid (PFOA) and perfluorooctanesulfonic acid (PFOS) in surface waters in 2001–2010 (a) and 2011–2020 (b). Figure taken from Podder et al. (2021). Copyright: 2021 Elsevier (reproduction with permission).

Muir and Miaz (2021) comprehensively analyzed spatiotemporal trends of PFAS in global surface waters (29,500 values), focusing on coastal seas, the Great Lakes, and open oceans, along with mass discharge estimates from major rivers (Figure 6). PFAS concentration in coastal seas and open oceans was orders of magnitude lower than that in inland surface waters (e.g., Figure 5), and ocean waters (e.g., 5,845 m depth) had the lowest PFAS concentrations (e.g., 11–69 pg/L in the Atlantic Ocean) (Miranda et al., 2021). In line with the trends observed above, the highest concentrations of PFAS, primarily including PFOS, PFOA, PFHxS, PFHxA, PFBS, and PFBA were reported in Asia (e.g., China Bohai and Yellow seas) and Europe (e.g., North and Baltic seas) (Figure 6) (Miranda et al., 2021; Muir and Miaz, 2021). Spatiotemporal analyses of PFAS concentrations showed a significant decline in PFSAs and C7–C12 PFCAs during 2012–2018 in China and European seas, as well as in the Great Lakes of

North America (Muir and Miaz, 2021). Due to the switching of using short-chain PFAS, the concentrations of C4–C6 PFCAs rapidly increased across the world after 2010, particularly in the Indian Ocean and the South Atlantic (Figure 6a). However, it may take several years or even decades to see a substantial reduction of C7–C12 PFCAs and PFSAs in oceans and seas (Figure 6b–c) due to the long residence time of PFAS in large open waters. Mass discharge estimates suggest a continued emission of long-chain C7–C12 PFCAs during 2015–2019 into major rivers in China; however, a reduced emission of long-chain PFCAs occurred into European rivers compared to earlier time periods (Figure 6). As expected, PFAS concentrations exhibit spatial and temporal variations among different water bodies (Muir and Miaz, 2021; Podder et al., 2021), and more periodic sampling and monitoring are needed to understand the fluxes, loading, transport, and transformation of PFAS compounds within and among different water systems.
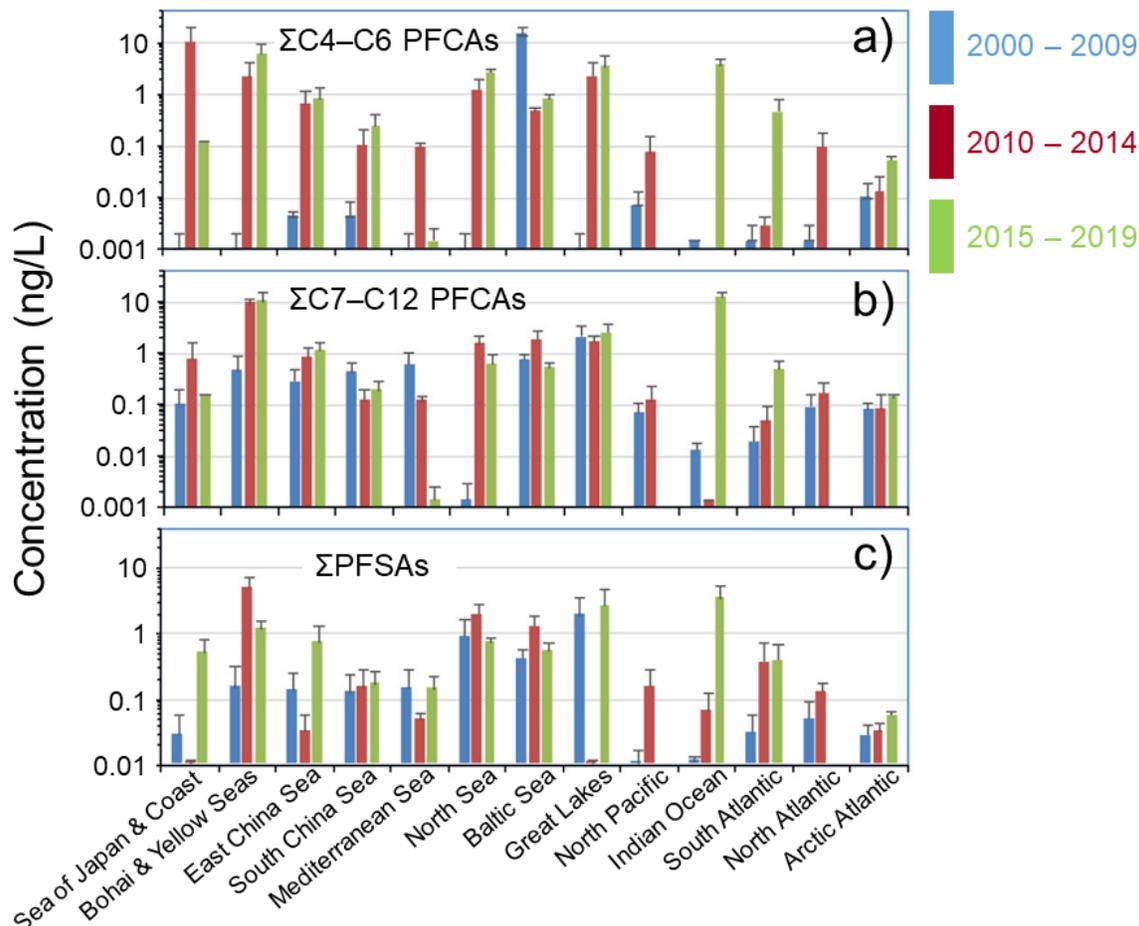
Figure 6. Global concentrations (ng/L) of ΣC4–C6 PFCAs (a), ΣC7–C12

18

PFCAs (b), and PFSAs (c) in coastal and ocean waters over three time periods of 2000–2009, 2010–2014, and 2015–2019. Median concentrations and absolute deviations are reported. Figure taken from Muir and Miaz (2021) (https:// pubs.acs.org/doi/full/10.1021/acs.est.0c08035). Copyright: 2021 American Chemical Society (reproduction with permission).

In general, PFAS concentration in groundwater is lower than that in surface water. For example, mean PFAS concentration in groundwater near the Nakdong River Basin is reported at 14.1 ng/L after a PFAS leakage incident in South Korea in 2018, which is lower than that in river water (44.8 ng/L) and tap water (58.9 ng/L) (Yong et al., 2021). Xu et al. (2021) recently reviewed the occurrence and concentration of PFAS in global groundwater systems, and reported that PFOS, PFOA, PFBA, PFBS, PFHxS, and PFNA are the most detected and abundant PFAS species. Mean concentrations of PFOS, PFOA, PFBA, PFBS, PFHxS, and PFNA ranged between 0–4,800, 0–4,150, 0–3,610, 0–865, 0–280, and 0–22 ng/L, respectively, with the highest PFAS levels occurring in China (e.g., Daling River Basin and fluorochemical industrial park) and Australia (Bores surrounding legacy landfills in Melbourne) (Xu et al., 2021). Recent surveys have also reported high concentrations of PFAS (~4,773 ng/L) in groundwater in the vicinity of PFAS manufacturing facility and reclaimed water recharge facility (Canez et al., 2021; Petre et al., 2021). Mass discharge of PFAS (e.g., 18–32 kg/year) into groundwater systems poses a long-term threat to drinking water sources and supplies (Petre et al., 2021).

High levels of PFAS have been increasingly reported in a wide range of environmental compartments in the vicinity of municipal and industrial disposal sites, legacy or contemporary AFFFs training sites, WWTPs, and landfills. The concentrations of 29 PFAS in groundwater and stream water ranged 20–4,773 and 426–3,617 ng/L, respectively, located near a PFAS manufacturing facility in North Carolina, USA (Petre et al., 2021). Concentrations of total PFAS and PFBS of up to 78,700 and 8,040 ng/L, respectively, have been reported from wastewater at electronic fabrication facilities (Jacob et al., 2021). These high concentrations of PFBS detected in the wastewater were likely associated with the use of photoacid generators during photolithography (Jacob et al., 2021). Mean concentrations of PFOS, PFHxS, PFHxA, PFOA, and 6:2 FTS were reported at 250, 230, 130, 70, and 90 ng/L, respectively, in surface waters near U.S. Air Force Bases with historical uses of AFFF formulations (East et al., 2021). PFAS concentrations in 10 different environmental media at 10 active U.S. Air Force installations reached 4,300 ng/L in groundwater and 8,970 ng/L in surface water (Anderson et al., 2016). Concentrations of PFOA, PFBA, PFOS, and PFBS in groundwater reached up to 21,200 ng/L (with GenX reaching 30,000 ng/L) near fluorochemical manufacturers in China (Xu et al., 2021). Some general trends on PFAS occurrence and concentration in the environment include: (1) higher PFAS concentrations are generally observed in summer with lower concentration occurring in winter, which is associated with water flow rates (Wang et al., 2019); and (2) runoff, precipitation, and snowmelt are also reported to strongly impact PFAS concentrations in surface waters (Miner et

al., 2021; Podder et al., 2021).

1.   PFAS in Soils

Short-chain PFAS tend to transport more rapidly and infiltrate into the groundwater, while long-chain PFAS are expected to be retained in surface soils by organic carbon, clays, and iron/aluminum oxides, particularly at the AWI (due to the hydrophobic interactions) (Leeson et al., 2021; Li et al., 2018). Strynar et al. (2012) in 2012 estimated that total global loadings of PFOA and PFOS are ~1,860 and ~7,080 metric tons, respectively, in surface soils (top 15 cm). Washington et al. (2019) in 2019 estimated that the summed loading of 8 PFAS (C6–C12) ranges from 1,500–9,000 metric tons with mean estimates of ~1,000 metric tons for C8 PFOA and PFOS. Overall, soil is regarded as one of the major reservoirs for PFOS, accounting for over 40% of the total mass of PFOS (Brusseau et al., 2020). Brusseau et al. (2020) recently conducted a global analysis of PFAS concentration in background and contaminated soils (25,000 soils). The analysis indicated that PFAS concentrations in contaminated soils are generally orders of magnitude higher than background levels (Brusseau et al., 2020). Specifically, total PFAS concentrations in soils without major contamination sources vary between <0.001 to 237 µg/kg, with PFOS (0.003–162 µg/kg) and PFOA (0.01–124 µg/kg) being most dominant PFAS species. In contrast, soil concentrations of PFOS concentrations in contaminated hotspots can reach up to 460,000 µg/kg with a median value of 8,722 µg/kg (PFOA are 50,000 and 83 µg/kg, respectively). These contaminated soils are adjacent to PFAS manufacturing plants, AFFFs-associated locations in airports and military installations, or associated with land applications of PFAS-impacted biosolids and irrigation of PFAS-contaminated water (Brusseau et al., 2020).

1. **Fate and Transport of PFAS in Subsurface Environment/Vadose Zone**

Evidence shows that transport of long-chain PFAS in subsurface environments is retarded (Davis et al., 2007; Emmett et al., 2006; Lindstrom et al., 2011; Xiao et al., 2015). For example, Xiao et al. (2015) reported elevated levels of PFAAs in soil and groundwater samples collected near a historical disposal site receiving PFAS-related industrial waste in the late 1940s 1950s. Weber et al. (2017) showed that PFAS contamination in the vadose zone continued to be a source of groundwater contamination for 18 years after training operations have ceased. These findings indicate that PFAS contamination sites with little or no control of PFAS-release to soils can constitute a source of groundwater contamination long after productions or disposal activities have ceased. This allows PFAS to have a long-term, long-range transport to the surrounding and deep soil-groundwater systems. Fate and transport of PFAS in subsurface environments are controlled by various processes, including adsorption to the solid–water interface (SWI) (Guelfo and Higgins, 2013; Higgins and Luthy, 2006), adsorption to the AWI in the unsaturated zone (Costanza et al., 2019; Lyu et al., 2018), and partitioning to NAPL or adsorption to NAPL–water interfaces in NAPL–contaminated source zones (Figure 3) (Brusseau, 2018; Guelfo and Higgins, 2013).

1. **Interactions with the Solid–Water Interface (SWI)**

    (a) Distribution and Organic Carbon (OC) Partition Coefficients

The sorption of PFAS to geosorbents is governed by hydrophobic and electrostatic interactions between the geosorbents and the PFAS molecules. PFAS chemicals vary in perfluoroalkyl chain lengths, molecular weights, molecular structures, and hydrophobicity (described above). These properties control the partitioning and adsorption propensities of PFAS in the environment (Mejia-Avendano et al., 2020; Nguyen et al., 2020; Zhou et al., 2013). The solid–water partition coefficient (K_d) and the organic carbon (OC) normalized distribution coefficient (K_{OC}) of PFAS have been used to evaluate the transport potential of PFAS in subsurface environments. To better understand the impact of PFAS properties on their transport, the relationship between the mean log K_d and log K_{OC} of anionic (e.g., PFCAs and PFSAs), zwitterionic, cationic, and nonionic PFAS was analyzed using data reported from field and laboratory studies (Figure 7) (Chen et al., 2020; Guelfo and Higgins, 2013; Mejia-Avendano et al., 2020; Nguyen et al., 2020). Similar to other organic compounds, the hydrophobic effects are associated with the molecular size or the length of perfluorinated carbon chain; each CF_2 moiety contributes 2.5–3.5 kJ/mol to the free energy of sorption (for kaolinite and sediments) (Higgins and Luthy, 2006; Xiao et al., 2011). Generally, short-chain PFAAs (N 5–7) exhibit similar K_d values, suggesting the minor role of carbon chain length in the sorption of short-chain PFAAs (Guelfo and Higgins, 2013; Nguyen et al., 2020). However, the K_d values for longer-chain PFAAs (N > 5–7) increase with increasing chain length (Figure 7a), signifying the key role of hydrophobicity for PFAS sorption (Chen et al., 2020; Guelfo and Higgins, 2013; Mejia-Avendano et al., 2020; Nguyen et al., 2020). For example, Zhou et al. (2013) observed a strong linear correlation between log K_{OC} and the chain length for C_8–C_{12} PFCAs (R = 0.79), but an almost invariable log K_{OC} value for short-chain PFCAs (N < 7) in a field study (sediment samples). A similar increase of log K_d with chain length for C_7–C_{10} PFCAs in different types of soils was also reported in a laboratory-based study (Guelfo and Higgins, 2013). Long-chain PFAAs (N > 6) display an increased retardation in soil, while short-chain PFAAs (N 6) generally show a rapid penetration through soil columns with no obvious retardation (McKenzie et al., 2015).

Compared to anionic PFAS, studies pertinent to the effects of chain length on the sorption and transport of novel PFAS (e.g., zwitterionic, cationic, and nonionic) are limited. Results showed that the sorption affinity of cationic and zwitterionic PFAS to sediment/soil is much stronger than that of anionic PFAS. Xiao et al. (2019) found that the K_d values of certain cationic and zwitterionic PFAS are several orders of magnitude greater than that of PFOA, but the difference tends to diminish with increasing concentration of PFAS. Nguyen et al. (2020) found that the K_d values of C6 zwitterionic PFAS are similar to those of C8 PFAS. A recent study also reported that, while the three

AFFF-related zwitterionic PFAS (AmPr-fluorohexanesulphone amide (FH_xSA), TAmPr-FH_xSA, and 6:2 FTSA-PrB) have six perfluorinated carbons, the K_d values of AmPr- and TAmPr-FH_xSA were 1–2 orders of magnitude larger than that of FTSA-PrB (Nguyen et al., 2020). This finding clearly suggests that functional group rather than the chain length likely controls the sorption of these zwitterionic PFAS.
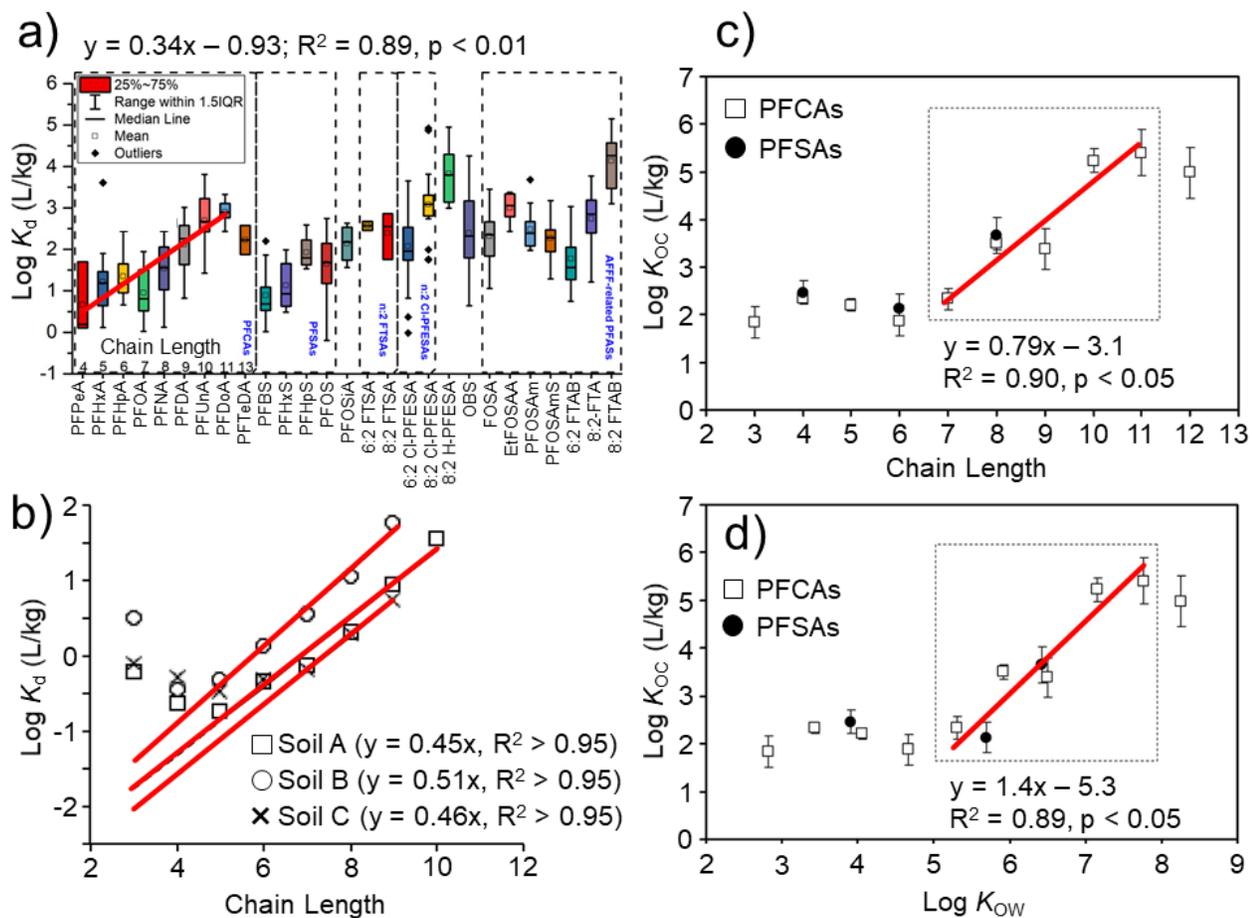

Figure 7. Mean $\log_{10} K_d$ (solid–water partition coefficient) and $\log_{10} K_{OC}$ (organic carbon normalized distribution coefficient) values of PFAS with different perfluorinated chain lengths based on field and laboratory data. Panels (a), (b), and (c–d) were modified from Chen et al. (2020), Guelfo and Higgins (2013), and Zhou et al. (2013), respectively. Copyrights: 2013 and 2020 American Chemical Society (reproduction with permission).

The $\log K_{OC}$ values vary among different PFAS classes (Figure 7). For anionic PFAS, $\log K_{OC}$ values of PFSAs are generally higher than those of PFCAs, although PFSAs and PFCAs have the same perfluoroalkyl chain length (Figure

7c–d). The average log K_{OC} values of PFSAs are 0.2–log units larger than those for PFCAs with an equivalent chain length in sediments (Figure 7a, c) (Zhou et al., 2013). Similar larger log K_{OC} values for PFSAs than PFCAs are also observed in different types of soils (Mejia-Avendano et al., 2020). This is mainly because carboxylate moiety has a smaller volume than sulfonate moiety, so PFCAs are slightly more hydrophilic and thus have a stronger sorption affinity to sediment/soil (Higgins and Luthy, 2006). Furthermore, the sorption affinity of cationic and zwitterionic PFAS to sediment/soil is much stronger with respect to that of anionic PFAS. Therefore, the sorption behavior of cationic/zwitterionic PFAS cannot be accurately predicted based on their hydrophobicity (Chen et al., 2020; Xiao et al., 2019). The K_d values of C6 zwitterionic PFAS are similar to those of C8 PFAS (Nguyen et al., 2020). The similar or slightly higher field-based log K_d values for certain cationic compounds than those of long-chain PFCAs in sediment are also reported (Chen et al., 2020). The more pronounced retardation of PFSAs than PFCAs with the same chain length during transport has been observed in soil-packed column studies (Gellrich et al., 2012; McKenzie et al., 2015). For example, Nickerson et al. (2021) found that zwitterionic and cationic PFAS show less transport potential compared to anionic PFAS. Therefore, in additional to the role of hydrophobic interaction, more studies are needed to identify the sorption mechanisms of different PFAS (anionic, cationic, and zwitterionic forms) on soils and sediments.

The adsorption of anionic PFAS is also driven by the surface charge of soils. Higher contents of iron (Fe) and aluminum (Al) oxides, coupled with lower soil pH (i.e., lower than the pK_a of Al and Fe oxides) produce an overall positively charged solid surface. This leads to the electrostatic attraction between the anionic PFAS and the solid surface (Campos-Pereira et al., 2020; Feng et al., 2017; Hellsing et al., 2016). Enhanced retardation of anionic PFAS during transport in soils with large OC and soil mineral contents (e.g., clays) is reported by Lyu et al. (2019).

For zwitterionic, cationic, and nonionic PFAS, a positive correlation of PFAS sorption/transport with soil organic matter (SOM) does not always occur (Barzen-Hanson et al., 2017b; Mejia-Avendano et al., 2020; Xiao et al., 2019). Mejia-Avendano et al. (2020) found that zwitterionic, cationic, and nonionic PFAS do not show any significant correlation between K_d and SOM. Similarly, Barzen-Hanson et al. (2017a) did not observe a significant correlation between the sorption of zwitterionic FtSaB and SOM. Xiao et al. (2019) also found that sorption of zwitterionic PFAS (PFOAB) correlates poorly with SOM, but sorption of cationic PFAS (PFOAAmS) correlates strongly with SOM. Partitioning of weakly hydrophobic organic cations in SOM is driven by cation exchange (MacKay and Seremet, 2008). Barzen-Hanson et al. (2017a) reported that the K_d value of 6:2 FTSA-PrB positively correlates with cation exchange capacity that considers the effect of H^+, Al^{3+}, and Mn^{2+} cations for highly acidic soils. A similar positive correlation with K_d and cation exchange capacity was also reported for cationic PFOAAmS (Mejia-Avendano et al., 2020; Xiao et al., 2019). However, the sorption of zwitterionic PFAS correlates poorly

23

with soil cation exchange capacity (Barzen-Hanson et al., 2017a; Xiao et al., 2019), but relates strongly with soil pH (Nguyen et al., 2020). With regard to nonionic PFAS, their sorption to soils is observed to correlate poorly with soil properties (Li et al., 2021), while organic matter may play an appreciable role. Further investigations are highly needed to elucidate how soil properties including organic matter affect the adsorption of nonionic PFAS in different soils and sediments.

In natural environments, the adsorption and transport behaviors of PFAS are determined by the complicated interplay between physicochemical characteristics of the PFAS and the soil properties, including both hydrophobic and electrostatics interactions. Therefore, multiple soil properties are more preferable than a single property to describe and predict the sorption behaviors of PFAS (Yan et al., 2020). Analyses using the multiple linear regression model showed that, the combination of organic carbon, silt-plus-clay content, and soil micropore volume can describe the sorption of anionic PFAS. In contrast, charged soil sites dominate the adsorption of zwitterionic PFAS, suggesting the dominant effect of electrostatic interactions on sorption of these zwitterions (Barzen-Hanson et al., 2017a; Nguyen et al., 2020). The above discussion clearly indicates that, the mobility of PFAS in the solid-water system can be predicted based on the length of perfluorinated chain, polarity, and functionality described above.

1. Effect of Solution Chemistry

Solution pH can affect the adsorption and transport of PFAS by changing both PFAS speciation and soil chemistry via surface complexation and electrostatic interaction which, in turn, alter the K_d values of PFAS (Nguyen et al., 2020). The pH-induced change in K_d values is due to the changes in the surface charge and/or hydrophobicity of the soil surfaces since pH change has little impact on the speciation of PFAS with low pK_a. At low pH, SOC is protonated and can enhance PFAS sorption through both hydrophobic and electrostatic attractions. With increasing pH, both SOC and clay minerals become more negatively charged, causing greater electrostatic repulsions between anionic PFAS and solid surface (i.e., reduced PFAS adsorption) (Gu et al., 1995). The reduced adsorption for anionic, zwitterionic, and nonionic PFAS having small pK_a with increasing solution pH in different matrixes has been widely reported (Higgins and Luthy, 2006; Nguyen et al., 2020; Oliver et al., 2019). For example, pK_a values of PFAAs and GenX are reported to be negative, and their log K_d values are reduced by 1–2 log units when pH is increased from ~3 to 8 (Nguyen et al., 2020). For PFAS with one large pK_a value, the overall surface charge switches from positive to neutral with increasing pH. At a given pH, the major speciation of PFAS compound determines the overall interaction with the solid surface. Zwitterionic PFAS compounds have different pK_a values and thus multiple chemical speciation states (e.g., anionic, neutral, or cationic speciation), which strongly affects their sorption.

Cations (e.g., Na^+, K^+, Mg^{2+}, and Ca^{2+}) can affect the adsorption and transport of PFAS via altering the electrostatic interactions. Increasing cation con-

centration is reported to increase the adsorption of anionic PFAS onto negatively charged solid surfaces, but decrease the adsorption of anionic PFAS onto positively charged solid surfaces (Tang et al., 2010; Wang and Shih, 2011; Zhao et al., 2014). Lyu et al. (2020b) further observed that high ionic strength significantly inhibits PFOA retention in water-saturated columns packed with positively charged sands. High ionic strength slightly increases PFOA retention in columns packed with negatively charged sands, as high ionic strength reduces the electrostatic repulsion between negatively charged sand surfaces and anionic PFOA molecules (Lyu et al., 2020b). On the other hand, inorganic cations may decrease the adsorption of cationic PFAS in geosorbents such as soils. To maintain electroneutrality, "native" cations (e.g., Na^+) of soils must be displaced by cationic PFAS (Xiao et al., 2019). For zwitterionic PFAS, Mejia-Avendano et al. (2020) found no discernible effect of Ca^{2+} (100 nM) on the adsorption of polyfluoroalkyl betaines in soils. Similarly, Xiao et al. (2019) also found that the effect of Na^+ on the sorption of a zwitterionic PFAS was insignificant. However, Li et al. (2011) reported that Ca^{2+} (300 mg/L) reduces the adsorption of the betaine-type hydrocarbon surfactants onto negatively charged quartz sand. The reported difference on PFAS adsorption is likely due to the difference of Ca^{2+} concentration selected. For cationic PFAS, Ca^{2+} affects their adsorption in an opposite trend compared to that for anionic PFAS (Mejia-Avendano et al., 2020). Increasing Ca^{2+} concentration causes a decrease in effective negative charges on soil surfaces. The electrostatic attraction between cationic PFAS and soil grains is reduced, leading to an increased adsorption of PFAAs. In summary, high ionic strength (cation concentration) likely favors the transport of anionic PFAS but inhibits the transport of cationic PFAS in subsurface environments.

1. **Interactions with the Air–Water Interface (AWI)**

A growing body of field studies have reported that the vadose zone acts as a significant reservoir for PFAS due to the strong interaction of PFAS with the AWI (Costanza et al., 2019; Schaefer et al., 2019; Silva et al., 2019). Brusseau (2018) reported that the adsorption of PFAS at the AWI can contribute ~50% of the total mass retained in unsaturated porous media. Recently, some research groups investigated the effect of AWI adsorption on PFAS transport using complementary strategies, including interfacial tension-based measurements, unsaturated column retardation methods, and batch system mass balance approaches (Costanza et al., 2019; Lyu et al., 2020b; Schaefer et al., 2019). The AWI partition coefficients (K_{ai}) measured experimentally are commonly used to assess the adsorption and retardation of PFAS during subsurface transport.

1. Effects of PFAS Property and Concentration

Current research efforts have focused primarily on the sorption of anionic PFAS (e.g., PFCAs and PFSAs) at the AWI. The K_{ai} values for PFCAs and PFSAs under different PFAS concentrations are shown in Figure 8. Apparently, the K_{ai} values for both PFCAs and PFSAs decrease with increasing PFAS concentrations (Figure 8a–b), suggesting the nonlinear adsorption of PFAS at the AWI. This coincides with the greater retardation of PFOA under a lower input

concentration in unsaturated sand packed columns (Lyu et al., 2018). Furthermore, for a specific PFAS type, the K_{ai} values are greater for the longer-chain (vs. shorter-chain) PFAS (Schaefer et al., 2019; Silva et al., 2019). Silva et al. (2019) systematically examined the correlation between K_{ai} values and chain length in deionized water and simulated groundwater containing $NaHCO_3$, $CaSO_4$, $MgSO_4$, and KCl. The authors observed that K_{ai} values exhibit a log-linearity with increasing chain length in deionized water (Silva et al., 2019). However, the log K_{ai} values in simulated groundwater showed a deviation from a log-linear trend with enhanced increase of K_{ai} with increasing carbon length ranging from 5 and 9 (Silva et al., 2019). This is likely due to: (1) the presence of dissolved ions in the solutions along with electrostatic effects at the AWI, (2) the enhancing free energy of air-water interfacial adsorption with increasing carbon length, and (3) the inherent differences in surface activity between odd and even homologues that are manifested more intensely when an excess of dissolved ions are present in solution (Lunkenheimer et al., 2015; Schaefer et al., 2019). When comparing PFCAs to PFSAs with both have the same chain length, the K_{ai} values for PFSAs are greater than PFCAs, indicating that the great role of head group for the air-water interfacial capacity (Brusseau, 2019; Brusseau and Van Glubt, 2019). Recent studies documented that the concentration at which the K_{ai} asymptotically approach their maximum values for GenX is higher than that for PFOA in the range of < 1 mg/L (Lyu et al., 2018; Yan et al., 2020). This suggests that PFOA exhibits a greater air-water interfacial activity compared to GenX. Brusseau (2019) examined the influence of molecular structure (e.g., molar volume and weight) on the adsorption of PFAS at the fluid-fluid interfaces. The molar volume is found to provide a reasonable representation of the effect of molecular size on cavity formation/destruction in solution, and thus the hydrophobic interaction driving force for the interfacial adsorption. A similar correlation between K_{ai} and molar volume was also observed by Schaefer et al. (2019) (Figure 8c).
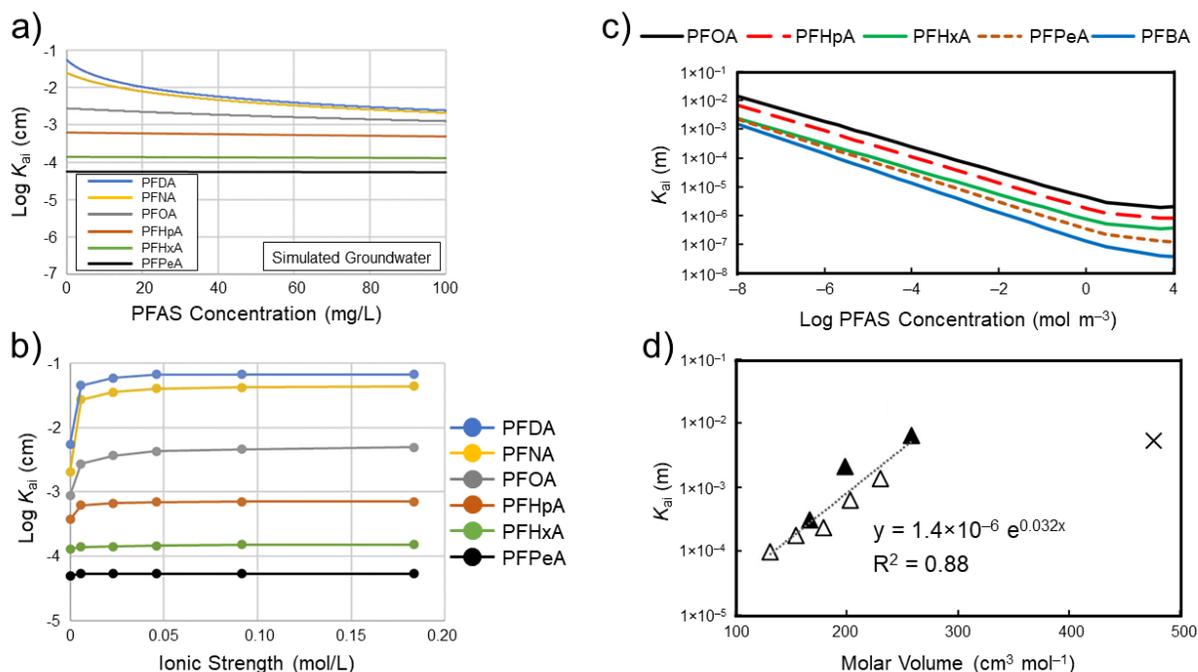
Figure 8. Calculated K_{ai} (partition coefficient at the air–water interface; AWI) for PFCAs and PFSAs as a function of PFAS concentration (a, c), ionic strength (b), and molar volume (d). Note different x- and y-axis units. Panels (a–b) were modified from Silva et al. (2019), and panels (c–d) were modified from Schaefer et al. (2019). Copyrights: 2019 Elsevier and 2019 American Chemical Society (reproduction with permission).

1.   Effect of Solution Chemistry

The sorption of PFAS at AWI was found to be strongly affected by the solution chemistry, including ionic strength, cation type, and pH (Brusseau and Van Glubt, 2019; Schaefer et al., 2019). Increasing ionic strength (e.g., NaCl and $CaCl_2$) greatly increases the accumulation of PFAS at the AWI. The addition of NaCl at concentrations of up to 0.01 M is reported to increase PFOS adsorption at the AWI by less than a factor of 2 at field relevant PFOS concentrations (Schaefer et al., 2019). Similarly, the presence of dissolved ions slightly increases the maximum surface excess for PFOA and PFOS (Costanza et al., 2019). This is because electrolyte ions (Na^+ and Ca^{2+}) can alleviate the electrostatic repulsion among PFAS headgroups at the AWI and increase the activity of the hydrophobic tail in solution, resulting in an increase in the driving force for PFAS adsorption (Brusseau and Van Glubt, 2019; Costanza et al., 2019). Greater retardation of PFOA during transport in unsaturated sand column with increasing ionic strength is also reported (Li et al., 2021; Lyu and Brusseau, 2020). For example, the retardation factor of PFOA increases gradu-

ally from 2.12 to 4.36 with the increase in ionic strength (1.5–30 mM NaCl) in sand column at an effective water saturation of 0.64.

The AWI sorption of PFAS is also impacted by the counterions, with greater K_{ai} values measured for counterions of smaller hydrated radii (Brusseau and Van Glubt, 2019; Lunkenheimer et al., 2015; Pottage et al., 2016; Zhao et al., 2010). Brusseau and Van Glubt (2019) found that surface activity is the lowest for Li-PFOA (with the largest hydrated radius) and the greatest for NH_4-PFOA (with a smaller hydrated radius). Pottage et al. (2016) reported that the change of counterion from ammonium to alkyl ammonium causes an enhancement in surface activity. This is likely because counterions with small radii are more likely to enter into the interfacial layer and reduce the electrostatic repulsion among PFOA headgroups, thus leading to a more compacted adsorbed monolayer and greater surface activity (Zhao et al., 2010). Li et al. (2021) further observed that the retardation of PFOA in unsaturated sand columns in the presence of Ca^{2+} is more pronounced than that for Na^+, due to the greater AWI adsorption in the presence of Ca^{2+}.

1. Interactions with NAPL–Water Interface (NWI)

PFAS retention processes may occur in NAPL–contaminated source zones, including partitioning into NAPL and adsorption at the NAPL–water interface (NWI) (Guelfo and Higgins, 2013; McKenzie et al., 2016; Van Glubt and Brusseau, 2021). Studies regarding PFAS adsorption and transport in the presence of AWI are limited, and most studies reported anionic PFAS, especially PFAAs. The impact of NAPL on the sorption of PFAAs to solids depends on the chain-length of PFAAs and their concentration. Guelfo and Higgins (2013) found that the effect of NAPL on the sorption of long-chain PFAAs (N > 6) is strongly dependent on the solid property and concentration of PFAAs, whereas the presence of NAPL increases the sorption of short-chain PFAAs (N 6) to all tested soils. This is likely because shorter-chain PFAAs fit better into the NAPL due to the less steric effect (Jonker et al., 2003). For long-chain PFAAs, the PFAAs at low concentrations may have access to an adequate number of high affinity sites on the solids, but they could also be segregated from sorption sites by NAPL, resulting in unchanged or slightly decreased sorption of PFAAs in the presence of NAPL. In contrast, NAPL may act as a sorbent to increase the overall sorption sites for PFAAs at high concentrations (increased sorption of PFAAs) (Guelfo and Higgins, 2013). In addition, SOC also has a great impact on PFAS sorption to solid surfaces in the presence of NAPL. The critical separate phase concentration is defined as the concentration (C_{NAPL}) where oil exists as a NAPL (typically at $1,000-3,000$ mg/kg) (Jonker et al., 2003; Ortiz et al., 1999), depending on the SOC because a NAPL will only form if the solid organic carbon is saturated with NAPL. So, a lower amount of NAPL is required to saturate the OC in solid with lower SOC. Once above the critical separate phase concentration, NAPL can serve as an additional sorbent either by bulk partitioning of PFAAs into NAPL or by adsorption of PFAAs to the NAPL–water interface to alter the sorption behaviors of PFAS (Guelfo

and Higgins, 2013; Jonker et al., 2003; Ortiz et al., 1999). It is observed that NAPL has a concentration-dependent effect on PFAAs sorption at lower SOC, whereas NAPL causes no change or decreases the sorption of PFAAs at higher SOC (Guelfo and Higgins, 2013).

The effect of NAPL on PFOA adsorption and transport was also examined through packed column experiments. McKenzie et al. (2016) found the retardation of PFAAs increases in trichloroethylene-containing columns, and PFAS partitioning into bulk NAPL and adsorption at the NAPL–water interface are interpreted as possible reasons for the observed enhanced retardation. Van Glubt, Brusseau, et al. (2019; 2021) further distinguished PFAS partitioning into the bulk NAPL and NAPL–water interfacial adsorption, and found that the adsorption to the NWI contributes to over 70–77% of the total retention of PFOS and PFOA.

Considering the significance of AWI and NWI on the adsorption of PFAS, Silva et al. (2019) further compared the adsorption capacity of PFCAs at these two interfaces (AWI and NWI in trichloroethylene and kerosene) (Figure 9). The authors observed that the values of K_{ni} (partition coefficient at the NAPL–water interface) were roughly 1–order of magnitude smaller than those of K_{ai} (partition coefficient at the AWI) for all PFCA homologues (Silva et al., 2019). This is likely due to the hydrophobic and oleophobic properties of perfluorocarbon tails of PFCAs. These perfluorocarbon tails tend to partition into the air-phase to minimize the overall free energy of the system. However, the orientation of perfluorocarbon tails positioned at the NWI is not clear, because the oleophobicity property of the tails limits their partitioning into the hydrocarbon phase. Altering NAPL saturation is expected to affect the retardation of PFCAs to a limited extent, as the area of NWI changes insignificantly for entrapped NAPL ganglia (Silva et al., 2019).
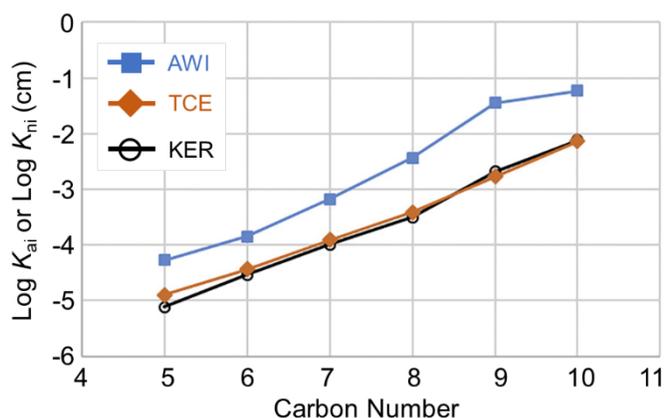
Figure 9. Comparison of $\log K_{ai}$ (partition coefficient at the air–water interface; AWI) and $\log K_{ni}$ (partition coefficient at the NAPL–water interface; NWI) relationships for AWI and NWI adsorption for 1 mg/L perfluorocarboxylic acid (PFCA) solution in simulated groundwater containing $NaHCO_3$, $CaSO_4$, $MgSO_4$, and KCl. TCE and KER refer to trichloroethene and kerosene, respectively. Figure taken from Silva et al. (2021). Copyright: 2019 Elsevier (reproduction with permission).

1. **Detailed PFAS Retention Mechanisms in Subsurface Environments**

The transport of PFAS in porous media is controlled by the sorption of PFAS on collector surfaces. PFAS typically have a C–F backbone and a nonfluorinated head consisting of a polar functional group. The head functional groups are normally polar and hydrophilic, such as carboxylic ($-COO^-$ in PFOA) and sulfonate functional groups ($-SO_3^-$ in PFOS). The tails of PFAS are hydrophobic and commonly lipophobic. Multiple retention mechanisms exist for PFAS in the subsurface due to the complex of environmental conditions (e.g., different grain surface charges, and in the presence of organic carbon, colloids, various interfaces such as the AWI) (Brusseau, 2018; Le et al., 2021; Wang et al., 2021). The major mechanisms controlling PFAS sorption on the environmental grain surfaces include electrostatic interaction, hydrophobic interaction, hydrogen bond, and ligand exchange (Figure 10) (Du et al., 2014; Liu et al., 2019; Wei et al., 2019).

Electrostatic interaction is considered as one of the major mechanisms controlling sorption and transport of PFAS in environmental media (Sharifan et al., 2021). The electrostatic interactions occur between the charged head functional groups of the PFAS and the mineral surfaces. Soil and aquifer grain surfaces frequently carry negative surface charges (e.g., due to isomorphous substitution) (Shen et al., 2020). Consequently, electrostatic repulsion exists between negatively charged PFAS and the negatively charged grain surfaces, favoring the transport of PFAS in the subsurface environments. However, the soil and aquifer grain surfaces often also contain positively charged minerals such as metal oxides or hydroxides (e.g., Fe and Al). PFAS will experience electrostatic attraction due to the positively charged minerals, which inhibits their transport in the subsurface (Figure 10). PFAS sorbed onto mineral surfaces can block subsequent sorption, thereby causing excess PFAS to become more mobile. Solution pH strongly influences the electrostatic interaction since it changes the net charges of the environmental grain surfaces and the functional groups of individual PFAS. Increasing solution ionic strength can reduce electrostatic attraction and repulsion due to charge screening effect, which decreases and increases the transport of PFAS in the subsurface environments, respectively (Tang et al., 2010). Xiao et al. (2011) showed that the electronegativity of PFAS may be not only because of their head functional groups. Furthermore, the C–F tail of PFAS molecules carry an excess negative surface charge due to the strong electronegativity of the fluoride atom.

30

Hydrophobic attraction exists when both interacting surfaces are hydrophobic (Figure 10). Therefore, the hydrophobic attraction facilitates the PFAS to be associated with the hydrophobic substances in subsurface environments such as organic carbon and organic contaminants (e.g., carbon nanotubes and chlorinated solvents) (Lyu et al., 2020a; 2020b). Because the AWI in the vadose zone is superhydrophobic, PFAS are favorable to be adsorbed on the AWI to form films, with the hydrophobic carbon-fluorine tail oriented toward the air and the hydrophilic head group dissolved in the water (Krafft and Riess, 2015; Lyu et al., 2018).

The hydrogen bond is a primarily electrostatic attraction force between a hydrogen (H) atom which is covalently bound to a more electronegative atom or group, and another electronegative atom owning a long pair of electrons (i.e., the hydrogen bond acceptor) (Figure 10) (Li et al., 2011b). When the adsorbent surfaces contain oxygen-containing functional groups such as –OH and –COOH, the hydrophilic O-containing functional groups of PFAS can form hydrogen bonds with the O-containing groups. Chen et al. (2015) examined the effects of PFOS and PFOA on bovine serum albumin by spectroscopic and molecular modeling. Through calculations of enthalpy and entropy change, the hydrogen bond was seen as one of the major forces causing the binding of the PFOS and PFOA to bovine serum albumin. Lu et al. (2016) examined the adsorption of PFOS on nanoparticles of Al_2O_3, Fe_2O_3, SiO_2, and TiO_2. They found that sulfonic functional group of PFOS formed hydrogen bonds with surfaces of the nanoparticles and the interaction was strongly dependent on solution pH. Gao and Chorover (2012) showed that hydrogen bond interactions existed between PFOS and hematite nanoparticles and water molecules competed with PFOS for adsorption on the nanoparticles via the hydrogen bond. Note that the carbon-fluorine tail chains are hydrophobic, which is difficult for them to form hydrogen bound with the oxygen on the functional groups of mineral surfaces (Du et al., 2014).

Ligand exchange is a chemical reaction in which a ligand (typically hydroxyl or water) in a compound is replaced by another (Figure 10). Ligand exchange also likely plays an important role in adsorption of PFAS on adsorbent surfaces through exchange of the surface functional groups on the adsorbent surfaces with the hydrophilic head functional groups the PFAS molecules. Gao and Chorover (2012) examined adsorption of PFOA on the iron oxide surfaces. They illustrated that the hydroxyl groups on the iron oxide surfaces can be replaced by the carboxyl groups of PFOA due to covalent metal-ligand bonding, leading to the formation of inner-sphere complexes:

$$Fe - \text{OH}_2^+ + C_7F_{15}COO^- \rightarrow Fe - OOF_{15}C_7 + H_2O \ (1)$$
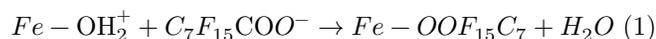
Gao and Chorover (2012) showed that while the PFOS, as mentioned previously, were adsorbed on hematite nanoparticle surfaces via hydrogen bond and electrostatic interaction (i.e., forming outer-sphere complexes of the PFOS sulfonate group with the nanoparticle surface sites), the adsorption of PFOA on the hematite nanoparticle surfaces was due to forming inner-sphere Fe-carboxylate

complexes by ligand exchange.

The long-range van der Waals interaction may only play a minor role in adsorption of PFAS. However, PFAS can aggregate into colloidal micelles at high concentrations, where the hydrophilic head portions interact with the water phase and the hydrophobic tail portions interaction with each other. In this case, the van der Waals force and the electrical double layer force may govern the interaction between the PFAS colloid and a collector surface (Molnar et al., 2015). These forces are quantitatively described by the Derjaguin–Landau–Verwey–Overbeek theory (Derjaguin and Landau, 1941; Verwey and Overbeek, 1948). Summing the two interaction forces/energies as a function of separation distance between the colloid and collector surface results in the interaction energy profiles of the Derjaguin–Landau–Verwey–Overbeek theory. The PFAS micelle colloids can be attached at the primary and/or secondary minima of the interaction energy profiles when both PFAS colloid and collector surfaces are negatively charged (Ryan and Elimelech, 1996; Shen et al., 2007; Shen et al., 2020). When the PFAS colloid and collector surfaces are oppositely charged, only primary minima exist on the interaction energy profiles and the PFAS colloids near the collector surfaces will be captured at the primary minima due to the attraction.
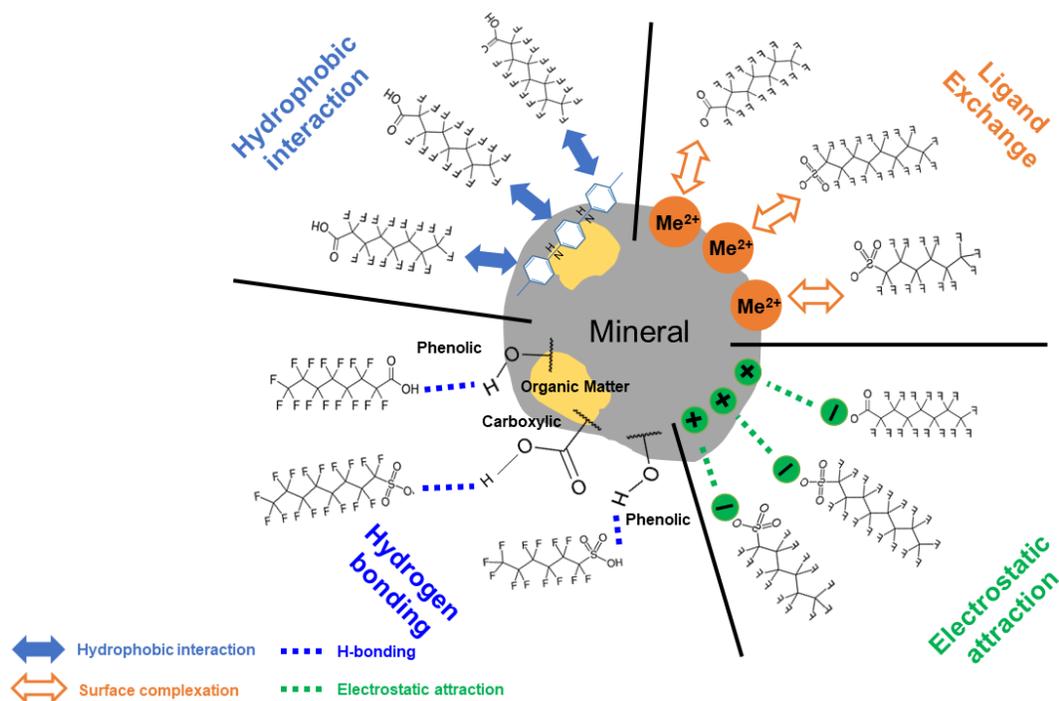

Figure 10. Schematic illustrating retention mechanisms of PFAS to soils or sediments in which mineral phase and organic matter dominate. PFOA with the carboxylic functional group (–COO⁻) and PFOS with the sulfonate functional

group ($-SO_3^-$) are shown as typical PFAS compounds.

1. **Modelling PFAS Transport in Subsurface Environments**

Understanding PFAS transport processes in subsurface environments including advection, dispersion, diffusion, and sorption is central for contaminated site management and remediation. Recently, numerical models accounting for PFAS-specific transport and retention processes, including surfactant-induced flow, rate-limited, nonlinear adsorption at the SWI and AWI, have been formulated (Abriola et al., 1993; Ji and Brusseau, 1998; Karagunduz et al., 2015). For example, a modified multi-process rate-limited mass-transfer (MPMT) model accounting for multiple retention processes, including adsorption at air-water and oil-water interfaces, adsorption by the solid phase, and diffusive mass-transfer between advective and non-advective domains was developed by Brusseau (2020) to simulate PFAS transport in the vadose zone. The multi-process model can simulate the transport of PFOA and PFOS under saturated and unsaturated porous media (Figure 11). The rate limitations associated with solid-phase adsorption and diffusive mass transfer between advective and non-advective domains are of great significance [Brusseau, 2020]. The four dimensionless governing equations are as follows (Brusseau, 2020):

$R_{a1}\frac{\partial C_a^*}{\partial T} + k_a^0\left(C_a^* - S_a^*\right) + \omega\left(C_a^* - C_n^*\right) = \frac{1}{P}\frac{\partial^2 C_a^*}{\partial X^2} - \frac{\partial C_a^*}{\partial X}$ (2)

$R_{n1}\frac{\partial C_n^*}{\partial T} + k_n^0\left(C_n^* - S_n^*\right) = \omega\left(C_a^* - C_n^*\right)$ (3)

$R_{a2}\frac{\partial S_n^*}{\partial T} = k_a^0\left(C_a^* - S_a^*\right)$ (4)

$R_{n2}\frac{\partial S_n^*}{\partial T} = k_n^0\left(C_n^* - S_n^*\right)$ (5)

where R_{a1} and R_{a2} are the retardation factors [–] in advective domain for the instantaneous rate-limited sorbed-phases, respectively; R_{n1} and R_{n2} are the retardation factors [–] in the non-advective domain for the instantaneous and rate-limited sorbed-phases, respectively; T is the time in pore volumes [–]; k_a^0 is the Damkohler number, representing contribution of sorption non-ideality in the advective domain [–]; k_n^0 is the Damkohler number, representing contribution of sorption non-ideality in the non-advective domain [–]; is the Damkohler number, representing the contribution of physical non-ideality (diffusive mass transfer between advective and nonadvective domains) [–]; P is the Peclet Number [–]; and X is the length [–].

Other parameters in Eqs. (1)–(4) are defined as follows (Brusseau, 2020):

$C_a^* = \frac{C_a}{C_0}$ (6)

$C_n^* = \frac{C_n}{C_0}$ (7)

$S_a^* = \frac{S_{a2}}{[(1-F_a)]K_a C_0}$ (8)

$S_n^* = \frac{S_{n2}}{[(1-F_n)]K_n C_0}$ (9)

where C_a is the solute concentration in the advective domain [M L^{-3}]; C_0 is the input solute concentration [M L^{-3}]; C_n is the solute concentration in the non-advective domain [M L^{-3}]; S_{a2} is the mass of sorbate in rate-limited sorbed-phase divided by the mass of sorbent in the advective domain [M M^{-1}]; F_a is the fraction of sorbent in the advective domain for which sorption is instantaneous [–]; k_a is the equilibrium sorption constant for the advective domain [L^3 M^{-1}]; S_{a2} is the mass of sorbate in rate-limited sorbed-phase divided by the mass of sorbent in the advective domain [M M^{-1}]; F_n is the fraction of sorbent in the non-advective domain for which sorption is instantaneous [–]; and K_n is the equilibrium sorption constant for the non-advective domain [L^3 M^{-1}].

The total retardation factor (R) is redefined as follows (Brusseau, 2020):

$$R = R_{a1} + R_{a2} + R_{n1} + R_{n2} = 1 + \frac{K_d \rho}{\theta} + \frac{K_{nw} A_{nw}}{\theta} \quad (10)$$

where K_d is the overall equilibrium sorption constant [L^3 M^{-1}]; K_{nw} is the fluid-fluid interfacial adsorption coefficient [L]; A_{nw} is the specific fluid-fluid interfacial area [L^2 L^{-3}];   is the bulk density [M L^{-3}];   is the volumetric water content [L^3 L^{-3}]; and   is the fraction of retardation associated with each domain, so the value of   = 1.

One simplified system is the case wherein physical nonideality is absent (either nonadvective pore water is absent or inter-domain mass transfer isnot rate limited), so solid-phase adsorption is rate limited, and fluid-fluid interfacial adsorption is also rate limited. The   term for this case is (Brusseau, 2020):

$$\beta_1 = \frac{R_{a1}}{R} = \frac{[1 + (\frac{\rho}{\theta}) F K_d]}{R} \quad (11)$$

$$\beta_2 = \frac{R_{a2}}{R} = \frac{[(\frac{\rho}{\theta})(1-F) K_d]}{R} \quad (12)$$

$$\beta_3 = \frac{R_{n1}}{R} = \frac{\left[\frac{K_{nw} A_{nw}}{\theta}\right]}{R} \quad (13)$$

$$\beta_4 = \frac{R_{n2}}{R} = 0 \quad (14)$$

where F is the fraction of sorbent in the advective domain for which sorption is instantaneous [–].

For a system with nonadvective domains (and the accompanying inter-domain diffusive mass transfer), rate-limited solid-phase adsorption, and assuming fluid-fluid interfacial adsorption to be effectively instantaneous, the   term is rewritten as follows (Brusseau, 2020):

$$\beta_1 = \frac{R_{a1}}{R} = \frac{\left[\phi + (f(\frac{\rho}{\theta}) F K_d) + \left(\phi \frac{K_{nw} A_{nw}}{\theta}\right)\right]}{R} \quad (15)$$

$$\beta_2 = \frac{R_{a2}}{R} = \frac{[f(\frac{\rho}{\theta})(1-F) K_d]}{R} \quad (16)$$

$$\beta_3 = \frac{R_{n1}}{R} = \frac{\left[(1-\phi) + ((1-f)(\frac{\rho}{\theta}) F K_d) + \left((1-\phi) \frac{K_{nw} A_{nw}}{\theta}\right)\right]}{R} \quad (17)$$

$$\beta_4 = \frac{R_{n2}}{R} = \frac{[(1-f)(\frac{\rho}{\theta})(1-F) K_d]}{R} \quad (18)$$

where equals to $_a/$ [–]; and f is the mass fraction of sorbent comprising the advective domain [–].
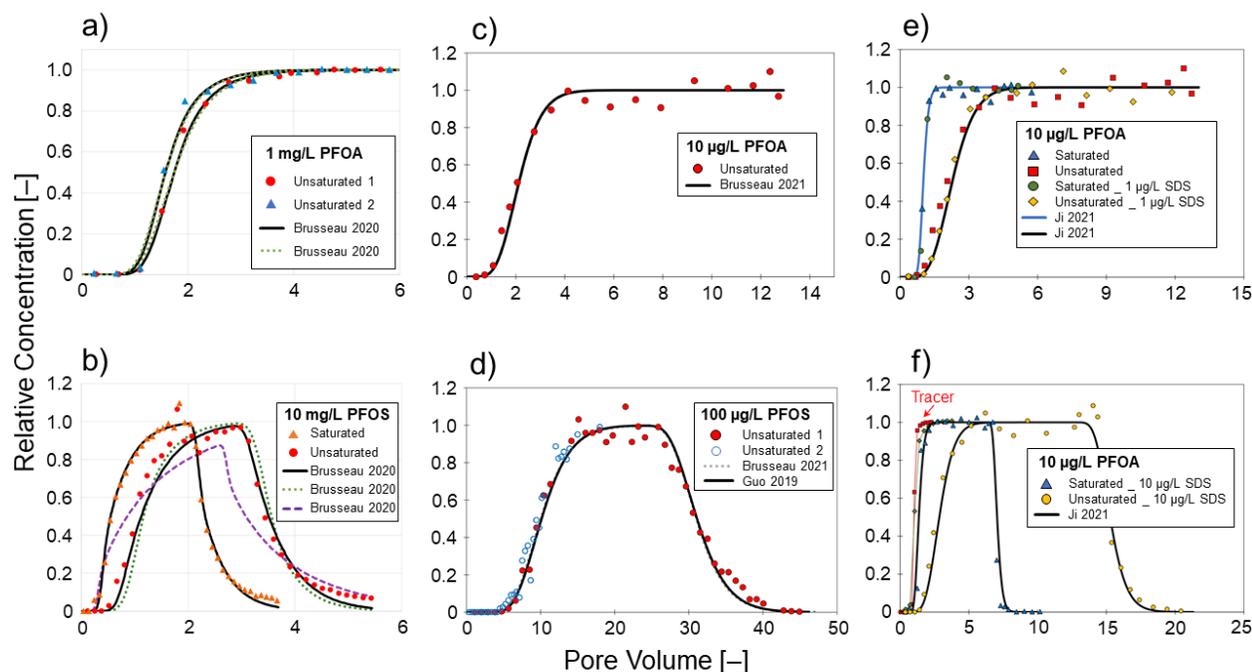

Figure 11. Measured (symbols) and fitted (lines) breakthrough curves of PFOA and PFOS in saturated and unsaturated porous media at the laboratory scale. The tested PFOA and PFOS concentrations ranged between 10 μg/L and 10 mg/L. The effective water saturation contents under unsaturated conditions ranged between 0.60 and 0.87. SDS refers to sodium dodecyl sulfate. The multi-process mass-transfer models, including Brusseau 2020 (a–b) (Brusseau 2020), Brusseau 2021 (c–d) (Brusseau et al., 2021), Guo 2019 (Guo et al., 2019), and Ji 2021 (e–f) (Ji et al., 2021) can describe the transport behaviors of PFAS under saturated and saturated porous media. Copyrights: 2020 Elsevier, 2021 Elsevier, and 2021 American Chemical Society (reproduction with permission).

1. **Challenges and Future Research Priorities and Recommendations**

There has been a substantial amount of research conducted on the fate and transport of PFAS in the environment during the past decades. The general transport mechanisms of PFAS, primarily including anionic PFAS compounds in subsurface media are well understood. Given the physicochemical characteristics of the PFAS and the properties of a subsurface porous media, retention and transport of PFAS can be estimated with models that have been developed. However, there is a large variety of different PFAS molecules, some of

which (e.g., cationic, zwitterionic, and nonionic PFAS) have not been characterized well, or just have been identified due to the development of analytical instrumentations (e.g., high resolution mass spectrometry) and reference standards (Wellington Laboratories Catologue, 2021). Furthermore, polyfluoroalkyl species can transform when they are exposed to environmental conditions. For instance, PFAS used as fire extinguishers or exposed to fires may transform into different forms of PFAS compounds. Critical knowledge gaps exist on the behavior, fate, and effects of newly identified cationic and zwitterionic PFAS in vadose and saturated zones. There is insufficient literature documenting the transport and retardation of these compounds in the subsurface soil and the aquifer. Detailed fate and transport studies are needed to understand the effects of solution chemistry, co-contaminants, soil properties, and other geologically relevant parameters and conditions on the fate and transport of novel PFAS in different geological settings.

Particularly, PFAS chemicals in surface soil may exposed to hot air in natural and engineered thermal remediation processes. One of the primary challenges in assessing the risk of soilborne PFAS to humans and wildlife is to better understand their fate in thermal processes such as fire training, biomass burning for land clearing, and natural wildfires. There were more than 57,000 wildfires in the U.S. in 2020 alone (Insurance Information Institute, 2020). The term "thermally stable" has been frequently used to describe PFAS in the literature, and fate and transport models generally rely on the assumption of high thermal stability of PFAS. The possible decomposition of soilborne PFAS and AFFF in thermal processes has received little attention or been overlooked altogether. A few recent studies by Xiao and collaborators have demonstrated that PFAS, including PFOA and PFOS, can be substantially decomposed when heated at moderate temperatures (e.g., 200 °C for PFOA and 500 °C for PFOS) (Sasi et al., 2021; Xiao et al., 2020; 2021). Thermal treatment likely alters the speciation of PFAS in soil. For example, the thermal decomposition of PFAAs and polyfluoroalkyl substances in laboratory tests yields various transient intermediates, including shorter-chained PFAAs (Sasi et al., 2021; Xiao et al., 2021). However, the long-term effect of thermal processes on the fate and transport of PFAS in surface and subsurface environments remains unclear, which is worthy of future study. Also, less research has been conducted with shorter-chained PFAS, and fate and transport of these PFAS in surface and subsurface environments remain a needed field of study. Additionally, the names of these newly identified PFAS can be readily obtained from the International Union of Pure and Applied Chemistry (IUPAC). However, there are inconsistencies in acronyms and terminology among different research groups. For example, fluorotelomer thioether amido sulfonate (FtTAoS) has been named as FTSAS in other studies (D'Agostino and Mabury, 2014). Harmonized acronyms and terminology for these emerging PFASs have not been established.

Given that a large portion of PFAS remain unidentified (Koelmel et al., 2021; Xiao, 2017), along with the heterogeneity and complexity of geological conditions, simple-to-use approaches for non-targeted or suspected screening of PFAS

need to be developed for identifying unknown PFAS as well as to evaluate PFAS degradation and transformation in the environment. To this end, software for PFAS compound analysis (e.g., FluoroMatch Flow 2.0) (Koelmel et al., 2021) that includes compound feather detection, mass matching, retention time pattern analysis, and fragment screening could accelerate identifying unknown PFAS in complicated environmental samples. However, transparency, collaboration, and coherence among academia, industry, government, and other stakeholders are the keys to share the hidden information on the environmental release of thousands of PFAS in the environment. A joint effort needs to be initiated to attempt to address this challenge.

PFAS are readily to bind with biomolecules such as proteins, transporters, and phospholipids, various *in vitro* and *in silico* approaches have been developed to facilitate parameterization of mechanistic models for risk assessment (De Silva et al., 2021). For example, *in vitro* methods such as cell- and vesicle-based assays can estimate PFAS uptake into cells via passive diffusion and active transport. *In silico* methods can predict PFAS behaviors in biological systems via high throughout testing, molecular docking, and molecular dynamics simulation (De Silva et al., 2021). Alternatively, classical quantitative-structure-activity relationship (QSAR) models can also provide insights into key physicochemical properties of PFAS for risk assessment (Lampic and Parnis, 2020). Computational strategies that integrate chemometrics (molecular dynamics simulation), machine learning (multitask neutral networks) (Cheng and Ng, 2019), statistics (QSAR), and bioinformatics (multi-omics) (Jiang et al., 2021; Lee et al., 2021) are needed to expedite risk assessment of a single as well as mixed PFAS compounds. A more standardized approach that can generate the needed information for the "big data" computational analyses is a prerequisite.

Managing and remediating PFAS contaminated sites remain largely challenging partly due to the persistence and recalcitrance of PFAS in subsurface environments. Complexity of geological media such as the presence of co-contaminants (e.g., NAPLs including petroleum hydrocarbons and possibly chlorinated solvents) further entangles the remedial processes and often compromises the remediation efficiency (Leeson et al., 2021; Silva et al., 2019). While various *ex situ* destruction techniques such as sonolysis, electrochemical oxidation, supercritical water oxidation, photocatalysis, and advanced reduction technology have shown promising results, most studies were performed at small laboratory scales with high treatment costs (Nzeribe et al., 2019). Field trials considering the impacts of NAPLs and hydrogeological and environmental parameters (e.g., water flow, redox condition, and presence of natural organic matter) need to be performed to evaluate the efficacy of different treatment techniques *in situ*. Sustainable and cost-effective techniques need to be pursed from the long-term perspective for contaminated site remediation.

Date Availability Statement

The data in Figure 4 were extracted from Brusseau and Glubt (2019), Silva et al. (2021), Vecitis et al. (2008), and Schaefer et al. (2019). The data in Figure

5 and Figure 6 were given in Podder et al. (2021), and Muir and Miaz (2021), respectively. The data in Figure 7 were given in Chen et al. (2020), Guelfo and Higgins (2013), and Zhou et al. (2013). The data in Figure 8 were given in Silva et al. (2019) and Schaefer et al. (2019) The data in Figure 9 were given in Silva et al. (2021). The data in Figure 11 were given in Brusseau (2020), Brusseau et al. (2021), and Ji et al. (2021).

Declaration of Interest

The authors declare that there is no conflict of interest.

1. **References**

Abriola, L. M., et al. (1993), Surfactant-enhanced solubilization of residual dodecane in soil columns. 2. Mathematical modeling, *Environmental Science & Technology*, *27*(12), 2341-2351.

Adamson, D. T., et al. (2020), Mass-based, field-scale demonstration of PFAS retention within AFFF-associated source areas, *Environmental Science & Technology*, *54*(24), 15768-15777.

Ahrens, L. (2011), Polyfluoroalkyl compounds in the aquatic environment: A review of their occurrence and fate, *Journal of Environmental Monitoring*, *13*(1), 20-31.

Anderson, R. H., et al. (2016), Occurrence of select perfluoroalkyl substances at US Air Force aqueous film-forming foam release sites other than fire-training areas: Field-validation of critical fate and transport properties, *Chemosphere*, *150*, 678-685.

Anderson, R. H., et al. (2019), Partitioning of poly-and perfluoroalkyl substances from soil to groundwater within aqueous film-forming foam source zones, *Journal of Contaminant Hydrology*, *20*, 59-65.

Arvaniti, O. S., & A. S. Stasinakis (2015), Review on the occurrence, fate and removal of perfluorinated compounds during wastewater treatment, *Science of the Total Environment*, *524-525*, 81-92.

ATSDR (2021), Toxicological Profile for Perfluoroalkyls, U.S. Department of Health and Human Services, Agency for Toxic Substances and Disease Registry (https://www.atsdr.cdc.gov/toxprofiles/tp200.pdf).

Backe, W. J., et al. (2013), Zwitterionic, cationic, and anionic fluorinated chemicals in aqueous film forming foam formulations and groundwater from U.S. military bases by nonaqueous large-volume injection HPLC-MS/MS, *Environmental Science & Technology*, *47*(10), 5226-5234.

Barry, V., et al. (2013), Perfluorooctanoic acid (PFOA) exposures and incident cancers among adults living near a chemical plant, *Environmental Health Perspectives*, *121*, 1313-1318.

Barton, C. A., et al. (2010), A site-specific screening comparison of modeled and monitored air dispersion and deposition for perfluorooctanoate, *Journal of the Air & Waste Management Association*, *60*(4), 402-411.

Barzen-Hanson, K. A., et al. (2017a), Sorption of fluorotelomer sulfonates, fluorotelomer sulfonamido betaines, and a fluorotelomer sulfonamido amine in national foam aqueous film-forming foam to soil, *Environmental Science & Technology*, *51*(21), 12394-12404.

Barzen-Hanson, K. A., et al. (2017b), Discovery of 40 classes of per- and polyfluoroalkyl substances in historical aqueous film-forming foams (AFFFs) and AFFF-impacted groundwater, *Environmental Science & Technology*, *51*(4), 2047-2057.

Bhhatarai, B., & P. Gramatica (2011), Prediction of aqueous solubility, vapor pressure and critical micelle concentration for aquatic partitioning of perfluorinated chemicals, *Environmental Science & Technology*, *45*(19), 8120-8128.

Bolan, N., et al. (2021), Distribution, behaviour, bioavailability and remediation of poly- and per-fluoroalkyl substances (PFAS) in solid biowastes and biowaste-treated soil, *Environment International*, *155*, 106600.

Borthakur, A., et al. (2021), Release of soil colloids during flow interruption increases the pore-water PFAS concentration in saturated soil, *Environmental Pollution*, *286*, 117297.

Brendel, S., et al. (2018), Short-chain perfluoroalkyl acids: environmental concerns and a regulatory strategy under REACH, *Environmental Sciences Europe*, *30*(1), 1-11.

Brusseau, M. L. (2018), Assessing the potential contributions of additional retention processes to PFAS retardation in the subsurface, *Science of the Total Environment*, *613-614*, 176-185.

Brusseau, M. L. (2019), The influence of molecular structure on the adsorption of PFAS to fluid-fluid interfaces: Using QSPR to predict interfacial adsorption coefficients, *Water Research*, *152*, 148-158.

Brusseau, M. L., & S. Van Glubt (2019), The influence of surfactant and solution composition on PFAS adsorption at fluid-fluid interfaces, *Water Research*, *161*, 17-26.

Brusseau, M. L., et al. (2019), Comprehensive retention model for PFAS transport in subsurface systems, *Water Research*, *148*, 41-50.

Brusseau, M. L. (2020), Simulating PFAS transport influenced by rate-limited multi-process retention, *Water Research*, *168*, 115179.

Brusseau, M. L., et al. (2020), PFAS concentrations in soils: Background levels versus contaminated sites, *Science of the Total Environment*, *740*, 140017.

Brusseau, M. L., et al. (2021), Ideal versus nonideal transport of PFAS in unsaturated porous media, *Water Research*, *202*, 117405.

Buck, R. C., et al. (2011), Perfluoroalkyl and polyfluoroalkyl substances in the environment: Terminology, classification, and origins, *Integrated Environmental Assessment and Management*, *7*(4), 513-541.

C8 Science Panel (2012), Probable Link Evaluation of Thyroid disease, *C8 Science Panel* (http://www.c8sciencepanel.org/pdfs/Probable_Link_C8_Thyroid_30Jul2012.pdf).

Campos-Pereira, H., et al. (2020), The adsorption of per- and polyfluoroalkyl Substances (PFASs) onto ferrihydrite is governed by surface charge, *Environmental Science & Technology*, *54*(24), 15722-15730.

Canez, T. T., et al. (2021), Perfluoroalkyl and polyfluoroalkyl substances (PFAS) in groundwater at a reclaimed water recharge facility, *Science of the Total Environment*, *791*, 147906.

Chen, H., et al. (2015), Systematic investigation of the toxic mechanism of PFOA and PFOS on bovine serum albumin by spectroscopic and molecular modeling, *Chemosphere*, *129*, 217-224.

Chen, H., et al. (2020), Occurrence and distribution of per- and polyfluoroalkyl substances in Tianjin, China: the contribution of emerging and unknown analogues, *Environmental Science & Technology*, *54*(22), 14254-14264.

Cheng, X., & C. A. Ng (2019), Using machine learning to classify bioactivity for 3486 per- and polyfluoroalkyl substances (PFASs) from the OECD list, *Environmental Science & Technology*, *53*(23), 13970-13980.

Costanza, J., et al. (2019), Accumulation of PFOA and PFOS at the air-water interface, *Environmental Science & Technology Letters*, *6*(8), 487-491.

D'Agostino, L. A., & S. A. Mabury (2014), Identification of novel fluorinated surfactants in aqueous film forming foams and commercial surfactant concentrates, *Environmental Science & Technology*, *48*(1), 121-129.

D'Agostino, L. A., & S. A. Mabury (2017), Certain perfluoroalkyl and polyfluoroalkyl substances associated with aqueous film forming foam are widespread in Canadian surface waters, *Environmental Science & Technology*, *51*(23), 13603-13613.

D'Ambro, E. L., et al. (2021), Characterizing the air emissions, transport, and deposition of per- and polyfluoroalkyl substances from a fluoropolymer manufacturing facility, *Environmental Science & Technology*, *55*(2), 862-870.

Darwin, R. L. (2011), Estimated inventory of PFOS-based aqueous film forming foam (AFFF), Fire Fighting Foam Coalition, Inc. Arlington, VA.

Davis, K. L., et al. (2007), Transport of ammonium perfluorooctanoate in environmental media near a fluoropolymer manufacturing facility, *Chemosphere*, *67*(10), 2011-2019.

De Silva, A. O., et al. (2021), PFAS exposure pathways for humans and wildlife: A synthesis of current knowledge and key gaps in understanding, *Environmental Toxicology and Chemistry*, *40*(3), 631-657.

Derjaguin, B., & L. Landau (1941), Theory of the stability of strongly charged lyophobic sols and of the adhension of strongly charged particles in solutions of electrolytes, *Acta Physicochim. URSS*, *14*, 733-762.

DOD (2017), Aqueous Film Forming Foam Report to Congress.

Dreyer, A., et al. (2010), Wet deposition of poly- and perfluorinated compounds in Northern Germany, *Environmental Pollution*, *158*(5), 1221-1227.

Du, Z., et al. (2014), Adsorption behavior and mechanism of perfluorinated compounds on various adsorbents--a review, *Journal of Hazardous Materials*, *274*, 443-454.

East, A., et al. (2021), Per- and polyfluoroalkyl Substances (PFAS) in surface water near US Air Force bases: Prioritizing individual chemicals and mixtures for toxicity testing and risk assessment, *Environmental Toxicology and Chemistry*, *40*(3), 859-870.

Emmett, E. A., et al. (2006), Community exposure to perfluorooctanoate: Relationships between serum concentrations and exposure sources, *Journal of Occupational and Environmental Medicine*, *48*(8), 759-770.

Fang, C., et al. (2019), Aggregated-fluorescent detection of PFAS with a simple chip, *Analytical Methods*, *11*(2), 163-170.

Feng, H., et al. (2017), In silico approach to investigating the adsorption mechanisms of short chain perfluorinated sulfonic acids and perfluorooctane sulfonic acid on hydrated hematite surface, *Water Research*, *114*, 144-150.

Fenton, S. E., et al. (2009), Analysis of PFOA in dosed CD-1 mice. Part 2. Disposition of PFOA in tissues and fluids from pregnant and lactating mice and their pups, *Reproductive Toxicology*, *27*, 365-372.

Field, J., et al. (2017), FAQs regarding PFASs associated with 15 AFFF use at U.S. military sites. Catalyzing rapid information transfer among key 16 stakeholders on per- and polyfluoroalkyl substances (PFASs) at contaminated military 17 sites. ESTCP project ER-201574-T2 Final Report., U.S. Department of Defense (DOD), Environmental Security Technology Certification Program (ESTCP).

Gao, X., & J. Chorover (2012), Adsorption of perfluorooctanoic acid and perfluorooctanesulfonic acid to iron oxide surfaces as studied by flow-through ATR-FIIR spectroscopy, *Environmental Chemistry*, *9*, 148-157.

Gellrich, V., et al. (2012), Behavior of perfluorinated compounds in soils during leaching experiments, *Chemosphere*, *87*(9), 1052-1056.

Ghisi, R., et al. (2019), Accumulation of perfluorinated alkyl substances (PFAS) in agricultural plants: A review, *Environmental Research*, *169*, 326-341.

Giesy, J., & K. Kannan (2001), Global distribution of perfluoroctane sulfonate in wildlife, *Environmental Science & Technology*, *35*(7), 1339-1342.

Gu, B., et al. (1995), Adsorption and desorption of different organic matter fractions on iron oxide, *Geochimica et Cosmochimica Acta*, *59*(2), 219-229.

Guelfo, J. L., & C. P. Higgins (2013), Subsurface Transport Potential of Perfluoroalkyl Acids at Aqueous Film-Forming Foam (AFFF)-Impacted Sites, *Environ. Sci. Technol.*, *47*(9), 4164-4171.

Guo, B., et al. (2019), A mathematical model for the release, transport, and retention of per- and polyfluoroalkyl substances (PFAS) in the vadose zone, *Water Resources Research*, *56*(2), e2019WR026667.

Hamid, H., et al. (2018), Review of the fate and transformation of per- and polyfluoroalkyl substances (PFASs) in landfills, *Environmental Pollution*, *235*, 74-84.

Hatton, J., et al. (2018), Occurrence and behavior of per-and polyfluoroalkyl substances from aqueous film-forming foam in groundwater systems, *Remediation Journal*, *28*(2), 89-99.

Hellsing, M. S., et al. (2016), Sorption of perfluoroalkyl substances to two types of minerals, *Chemosphere*, *159*, 385-391.

Heydebreck, F., et al. (2015), Alternative and legacy perfluoroalkyl substances: Differences between European and Chinese river/estuary systems, *Environmental Science & Technology*, *49*(14), 8386-8395.

Higgins, C. P., et al. (2005), Quantitative determination of perfluorochemicals in sediments and domestic sludge, *Environ. Sci. Technol.*, *39*(11), 3946–3956.

Higgins, C. P., and R. G. Luthy (2006), Sorption of perfluorinated surfactants on sediments, *Environ. Sci. Technol.*, *40*(23), 7251-7256.

Hogue, C. (2021), US PFAS makers will have to control releases to water, CE&N News, September, ACS, Washington DC.

Houtz, E. F., et al. (2013), Persistence of perfluoroalkyl acid precursors in AFFF-impacted groundwater and soil, *Environmental Science & Technology*, *47*(15), 8187-8195.

Insurance Information Institute (2020), Wildfire statistics, *Insurance Information Institute,* https://www.iii.org/fact-statistic/facts-statistics-wildfires.

ITRC (2020), PFAS - Per- and polyfluoroalkyl substances, The Interstate Technology & Regulatory Council (ITRC).

Jacob, P., et al. (2021), Target and nontarget analysis of per- and polyfluoralkyl substances in wastewater from electronics fabrication facilities, *Environmental Science & Technology*, *55*(4), 2346-2356.

Ji, W., & M. L. Brusseau (1998), A general mathematical model for chemical-enhanced flushing of soil contaminated by organic compounds, *Water Resources Research*, *34*, 1635-1648.

Ji, Y., et al. (2021), Impact of a hydrocarbon surfactant on the retention and transport of perfluorooctanoic acid in saturated and unsaturated porous media, *Environmental Science & Technology*, *55*(15), 10480-10490.

Jiang, L., et al. (2021), Comprehensive multi-omics approaches reveal the hepatotoxic mechanism of perfluorohexanoic acid (PFHxA) in mice, *Science of the Total Environment*, *790*, 148160.

Jin, B., et al. (2020), In vivo generation of PFOA, PFOS, and other compounds from cationic and zwitterionic per- and polyfluoroalkyl substances in a terrestrial invertebrate (Lumbricus terrestris), *Environmental Science & Technology*, *54*(12), 7378-7387.

Jonker, M. T. O., et al. (2003), Sorption of polycyclic aromatic hydrocarbons to oil contaminated sediment: Unresolved complex?, *Environmental Science & Technology*, *37*(22), 5197-5203.

Kallenborn, R. (2004), Perfluorinated alkylated substances (PFAS) in the Nordic environment, Nordic Council of Ministers.

Karagunduz, A., et al. (2015), Influence of surfactants on unsaturated water flow and solute transport, *Water Resources Research*, *51*(4), 1977-1988.

Koelmel, J. P., et al. (2021), FluoroMatch 2.0—making automated and comprehensive non-targeted PFAS annotation a reality, *Analytical and Bioanalytical Chemistry*, DOI: 10.1007/s00216-021-03392-7.

Krafft, M. P., & J. G. Riess (2015), Selected physicochemical aspects of poly- and perfluoroalkylated substances relevant to performance, environment and

sustainability-Part one, *Chemosphere*, *129*, 4-19.

Lakshminarasimman, N., et al. (2021), Removal and formation of perfluoroalkyl substances in Canadian sludge treatment systems – A mass balance approach, *Science of the Total Environment*, *754*, 142431.

Lampic, A., & J. M. Parnis (2020), Property estimation of per- and polyfluoroalkyl substances: A comparative assessment of estimation methods, *Environmental Toxicology and Chemistry*, *39*(4), 755-786.

Lazcano, R., et al. (2019), Per- and polyfluoroalkyl substances in commercially available biosolid-based products: The effect of treatment processes, *Water Environment Research*, *91*, 1669-1677.

Le, S., et al. (2021), A group-contribution model for predicting the physicochemical behavior of PFAS components for understanding environmental fate, *Science of the Total Environment*, *764*, 142882.

Lee, H., et al. (2021), Integrated multi-omics analysis reveals the underlying molecular mechanism for developmental neurotoxicity of perfluorooctanesulfonic acid in zebrafish, *Environment International*, *157*, 106802.

Leeson, A., et al. (2021), Identifying and managing aqueous film-forming foam-derived per- and polyfluoroalkyl substances in the environment, *Environmental Toxicology and Chemistry*, *40*(1), 24-36.

Lenka, S. P., et al. (2021), A review of the occurrence, transformation, and removal of poly- and perfluoroalkyl substances (PFAS) in wastewater treatment plants, *Water Research*, *199*, 117187.

Li, F., et al. (2020), Short-chain per-and polyfluoroalkyl substances in aquatic systems: Occurrence, impacts and treatment, *Chemical Engineering Journal*, *380*, 122506.

Li, L., et al. (2015), Estimating industrial and domestic environmental releases of perfluorooctanoic acid and its salts in China from 2004 to 2012, *Chemosphere*, *129*, 100-109.

Li, N., et al. (2011a), Adsorption behavior of betaine-type surfactant on quartz sand, *Energy & Fuels*, *25*(10), 4430-4437.

Li, Y., et al. (2018), A critical analysis of published data to discern the role of soil and sediment properties in determining sorption of per and polyfluoroalkyl substances (PFASs), *Science of the Total Environment*, *628-629*, 110-120.

Li, Z., et al. (2011b), Quantum nature of the hydrogen bond, *Proceedings of the National Academy of Sciences of the United States of America*, *108*, 6369-6373.

Li, Z., et al. (2021), Effects of ionic strength and cation type on the transport of perfluorooctanoic acid (PFOA) in unsaturated sand porous media, *J. Hazardous Materials*, *403*, 123688.

Lindstrom, A. B., et al. (2011), Application of WWTP biosolids and resulting perfluorinated compound contamination of surface and well water in Decatur, Alabama, USA, *Environmental Science & Technology*, *45*(19), 8015-8021.

Liu, L., et al. (2019), Removal of perfluorooctanoic acid (PFOA) and perfluorooctane sulfonate (PFOS) from water by carbonaceous nanomaterials: A review, *Critical Reviews in Environmental Science and Technology*, *50*(22), 2379-2414.

Lu, X., et al. (2016), Adsorption behavior and mechanism of perfluorooctane sulfonate on nanosized inorganic oxides, *Journal of Colloid and Interface Science*, *474*, 199-205.

Lunkenheimer, K., et al. (2015), Adsorption properties of surface chemically pure sodium perfluoro-n-alkanoates at the air/water interface: counterion effects within homologous series of 1:1 ionic surfactants, *Langmuir*, *31*(3), 970-981.

Luo, Y. S., et al. (2020), Rapid characterization of emerging per- and polyfluoroalkyl substances in aqueous film-forming foams using ion mobility spectrometry–mass spectrometry, *Environmental Science & Technology*, *54*(23), 15024-15034.

Lyu, X., et al. (2019), Transport and retention of perfluorooctanoic acid (PFOA) in natural soils: Importance of soil organic matter and mineral contents, and solution ionic strength, *Journal of Contaminant Hydrology*, *225*, 103477.

Lyu, X., et al. (2020a), Importance of surface roughness on perfluorooctanoic acid (PFOA) transport in unsaturated porous media, *Environmental Pollution*, *226*, 115343.

Lyu, X., et al. (2020b), Importance of Al/Fe oxyhydroxide coating and ionic strength in perfluorooctanoic acid (PFOA) transport in saturated porous media, *Water Research*, *175*, 115685.

Lyu, Y., et al. (2018), Adsorption of PFOA at the air-water interface during transport in unsaturated porous media, *Environmental Science & Technology*, *52*(14), 7745-7753.

Lyu, Y., & M. L. Brusseau (2020), The influence of solution chemistry on air-water interfacial adsorption and transport of PFOA in unsaturated porous media, *Science of the Total Environment*, *713*, 136744.

MacKay, A. A., & D. E. Seremet (2008), Probe compounds to quantify cation exchange and complexation interactions of ciprofloxacin with soils, *Environmental Science & Technology*, *42*(22), 8270-8276.

McGregor, R., & Y. Zhao (2021), The in situ treatment of TCE and PFAS in groundwater within a silty sand aquifer, *Remediation Journal*, *31*, 7-17.

McKenzie, E. R., et al. (2015), Effects of chemical oxidants on perfluoroalkyl acid transport in one-dimensional porous media columns, *Environmental Science & Technology*, *49*(3), 1681-1689.

McKenzie, E. R., et al. (2016), The influence of a non-aqueous phase liquid (NAPL) and chemical oxidant application on perfluoroalkyl acid (PFAA) fate and transport, *Water Research*, *92*, 199-207.

Mejia-Avendano, S., et al. (2016), Generation of perfluoroalkyl acids from aerobic biotransformation of quaternary ammonium polyfluoroalkyl surfactants, *Environmental Science & Technology*, *50*(18), 9923-9932.

Mejia-Avendano, S., et al. (2020), Sorption of polyfluoroalkyl surfactants on surface soils: Effect of molecular structures, soil properties, and solution chemistry, *Environmental Science & Technology*, *54*(3), 1513-1521.

Miner, K. R., et al. (2021), Deposition of PFAS 'forever chemicals' on Mt. Everest, *Science of the Total Environment*, *759*, 144421.

Miranda, D. D. A., et al. (2021), Perfluoroalkyl substances in the western tropical Atlantic ocean, *Environmental Science & Technology*, DOI: 10.1021/acs.est.1c01794.

Molnar, I. L., et al. (2015), Predicting colloid transport through saturated porous media: A critical review, *Water Resources Research*, *51*, 6804-6845.

Moodie, D., et al. (2021), Legacy and emerging per- and polyfluoroalkyl substances (PFASs) in Australian biosolids, *Chemosphere*, *270*, 129143.

Moody, C. A., et al. (2002), Monitoring perfluorinated surfactants in biota and surface water samples following an accidental release of fire-fighting foam into Etobicoke Creek, *Environmental Science & Technology*, *36*(4), 545-551.

Morales-McDevitt, M. E., et al. (2021), The air that we breathe: Neutral and volatile PFAS in indoor air, *Environmental Science & Technology Letters*, DOI: 10.1021/acs.estlett.1c00481.

Muir, D., & L. T. Miaz (2021), Spatial and temporal trends of perfluoroalkyl substances in global ocean and coastal waters, *Environmental Science & Technology*, *55*(14), 9527-9537.

Nguyen, T. M. H., et al. (2020), Influences of chemical properties, soil properties, and solution pH on soil-water partitioning coefficients of per- and polyfluoroalkyl substances (PFASs), *Environmental Science & Technology*, *54*(24), 15883-15892.

Nickerson, A., et al. (2021), Spatial trends of anionic, zwitterionic, and cationic PFASs at an AFFF-impacted site, *Environmental Science & Technology*, *55*(1), 313-323.

Nzeribe, B. N., et al. (2019), Physico-chemical processes for the treatment of per-and polyfluoroalkyl substances (PFAS): A review, *Critical Reviews in Environmental Science and Technology*, *49*(10), 866-915.

OECD (2018), Toward a New Comprehensive Global Database of Per-and Polyfluoroalkyl Substances (PFASs): Summary Report on Updating the OECD

2007 List of per-and Polyfluoroalkyl Substances (PFASs), Organisation for Economic Co-operation Development.

Oliver, D. P., et al. (2019), The role of surface charge and pH changes in tropical soils on sorption behaviour of per- and polyfluoroalkyl substances (PFASs), *Science of the Total Environment*, *673*, 197-206.

Ortiz, E., et al. (1999), Organic phase resistance to dissolution of polycyclic aromatic hydrocarbon compounds, *Environmental Science & Technology*, *33*(2), 235-242.

Petre, M. A., et al. (2021), Per- and polyfluoroalkyl substance (PFAS) transport from groundwater to streams near a PFAS manufacturing facility in North Carolina, USA, *Environmental Science & Technology*, *55*(9), 5848-5856.

Podder, A., et al. (2021), Per and poly-fluoroalkyl substances (PFAS) as a contaminant of emerging concern in surface water: A transboundary review of their occurrences and toxicity effects, *Journal of Hazardous Materials*, *419*, 126361.

Post, G. B. (2021), Recent US state and federal drinking water guidelines for per- and polyfluoroalkyl substances, *Environmental Toxicology and Chemistry*, *40*(3), 550-563.

Pottage, M. J., et al. (2016), The effects of alkylammonium counterions on the aggregation of fluorinated surfactants and surfactant ionic liquids, *Journal of Colloid and Interface Science*, *475*, 72-81.

Ruyle, B. J., et al. (2021a), Isolating the AFFF signature in coastal watersheds using oxidizable PFAS precursors and unexplained organofluorine, *Environmental Science & Technology*, *55*(6), 3686-3695.

Ruyle, B. J., et al. (2021b), Reconstructing the composition of per- and polyfluoroalkyl substances in contemporary aqueous film-forming foams, *Environmental Science & Technology Letters*, *8*(1), 59-65.

Ryan, J. N., & M. Elimelech (1996), Colloid mobilization and transport in groundwater, *Colloids and Surfaces A: Physicochemical and Engineering Aspects*, *107*, 1-56.

Sasi, P. C., et al. (2021), Effect of granular activated carbon and other porous materials on thermal decomposition of per- and polyfluoroalkyl substances: Mechanisms and implications for water purification, *Water Research*, *200*, 117271.

Schaefer, C. E., et al. (2019), Uptake of poly- and perfluoroalkyl substances at the air-water interface, *Environmental Science & Technology*, *53*(21), 12442-12448.

Schlummer, M., et al. (2013), Detection of fluorotelomer alcohols in indoor environments and their relevance for human exposure, *Environment International*, *57-58*, 42-49.

Schroeder, T., et al. (2021), PFAS soil and groundwater contamination via industrial airborne emission and land deposition in SW Vermont and Eastern New York State, USA, *Environmental Science: Processes & Impacts*, *23*, 291-301.

Scott, B. F., et al. (2006), Poly and perfluorinated carboxylates in North American precipitation, *Environmental Science & Technology*, *40*(23), 7167-7174.

Sepulvado, J. G., et al. (2011), Occurrence and fate of perfluorochemicals in soil following the land application of municipal biosolids, *Environmental Science & Technology*, *45*(19), 8106-8112.

SERDP-ESTCP (2017), SERDP and ESTCP workshop on research and demonstration needs for management of AFFF-impacted sites.

Sharifan, H., et al. (2021), Fate and transport of per- and polyfluoroalkyl substances (PFASs) in the vadose zone, *Science of the Total Environment*, *771*, 145427.

Shen, C., et al. (2007), Kinetics of coupled primary- and secondary-minimum deposition of colloids under unfavorable chemical conditions, *Environmental Science & Technology*, *41*, 6976-6982.

Shen, C., et al. (2020), Role and importance of surface heterogeneity in transport of particles in saturated porous media, *Critical Reviews in Environmental Science and Technology*, *50*, 244-329.

Shimizu, M. S., et al. (2021), Atmospheric deposition and annual flux of legacy perfluoroalkyl substances and replacement perfluoroalkyl ether carboxylic acids in Wilmington, NC, USA, *Environmental Science & Technology Letters*, *8*(5), 366-372.

Silva, J. A., et al. (2021), Air-water interfacial adsorption coefficients for PFAS when present as a multi-component mixture, *Journal of Contaminant Hydrology*, *236*, 103731.

Silva, J. A. K., et al. (2019), Evaluating air-water and NAPL-water interfacial adsorption and retention of perfluorocarboxylic acids within the vadose zone, *Journal of Contaminant Hydrology*, *223*, 103472.

Sima, M. W., & P. R. Jaffe (2021), A critical review of modeling poly- and perfluoroalkyl substances (PFAS) in the soil-water environment, *Science of the Total Environment*, *757*, 143793.

Simcik, M. F., & K. J. Dorweiler (2005), Ratio of perfluorochemical concentrations as a tracer of atmospheric deposition to surface waters, *Environmental Science & Technology*, *39*(22), 8678-8683.

Strynar, M. J., et al. (2012), Pilot scale application of a method for the analysis of perfluorinated compounds in surface soils, *Chemosphere*, *86*(3), 252-257.

Sun, H., et al. (2011), Long-chain perfluorinated chemicals in digested sewage sludges in Switzerland, *Environmental Pollution*, *159*, 654-662.

Sun, M., et al. (2016), Legacy and emerging perfluoroalkyl substances are important drinking water contaminants in the Cape Fear river watershed of North Carolina, *Environmental Science & Technology Letters*, *3*(12), 415-419.

Sunderland, E. M., et al. (2019), A review of the pathways of human exposure to poly- and perfluoroalkyl substances (PFASs) and present understanding of health effects, *Journal of Exposure Science & Environmental Epidemiology*, *29*, 131-147.

Tajima, K., et al. (1979), Surface activity of complex in mixed surfactant solution, *Bulletin of the Chemical Society of Japan*, *52*(7), 2060-2063.

Tang, C. Y., et al. (2010), Effect of solution chemistry on the adsorption of perfluorooctane sulfonate onto mineral surfaces, *Water Research*, *44*, 2654-2662.

USEPA (2009), Long-Chain Perfluorinated Chemicals (PFCs) Action Plan, U.S. Environmental Protection Agency (EPA).

USEPA (2014), Emerging Contaminants – Perfluorooctane Sulfonate (PFOS) and Perfluorooctanoic Acid (PFOA), Emerging Contaminants Fact Sheet – PFOS and PFOA, EPA 505-F-14-001., U.S. Environmental Protection Agency (EPA).

USEPA (2016a), Drinking water health advisory for perfluorooctanoic acid (PFOA). EPA 822-R-16-005, United States Environmental Protection (EPA), Office of Water, Washington, DC.

USEPA (2016b), Drinking water health advisory for perfluorooctane sulfonate (PFOS). EPA 822-16-004, United States Environmental Protection (EPA), Office of Water, Washington, DC.

USEPA (2018), Part 503 - Standards for the use or disposal of sewage sludge, U.S. Environmental Protection Agency (EPA).

USGAO (2018), Status of DOD efforts to address drinking water contaminants used in firefighting foam, U.S. Government Accountability Office (https://www.gao.gov/assets/700/694759.pdf).

Van Glubt, S., & M. L. Brusseau (2021), Contribution of nonaqueous-phase liquids to the retention and transport of per and polyfluoroalkyl substances (PFAS) in porous media, *Environmental Science & Technology*, *55*(6), 3706-3715.

Vecitis, C., et al. (2008), Enhancement of perfluorooctanoate and perfluorooctanesulfonate activity at acoustic cavitation bubble interfaces, *Journal of Physical Chemistry C*, *112*(43), 16850-16857.

Venkatesan, A. K., & R. U. Halden (2013), National inventory of perfluoroalkyl substances in archived US biosolids from the 2001 EPA National Sewage Sludge

Survey, *Journal of Hazardous Materials*, *252*, 413-418.

Verwey, E. J. M., & J. T. G. T. Overbeek (1948), Theory of the Stability of Lyophobic Colloids, Elsevier: Amsterdam, The Netherlands.

Wang, F., & K. M. Shih (2011), Adsorption of perfluorooctanesulfonate (PFOS) and perfluorooctanoate (PFOA) on alumina: Influence of solution pH and cations, *Water Research*, *45*(9), 2925-2930.

Wang, M., et al. (2021), Enhanced adsorption of per- and polyfluoroalkyl substances (PFAS) by edible, nutrient-amended montmorillonite clays, *Water Research*, *188*, 116534.

Wang, T., et al. (2015), A review of sources, multimedia distribution and health risks of perfluoroalkyl acids (PFAAs) in China, *Chemosphere*, *129*, 87-99.

Wang, Y., et al. (2019), A review of sources, multimedia distribution and health risks of novel fluorinated alternatives, *Ecotoxicology and Environmental Safety*, *182*, 109402.

Wang, Z., et al. (2017), A never-ending story of per- and polyfluoroalkyl substances (PFASs)?, *Environmental Science & Technology*, *51*(5), 2508-2518.

Washington, J. W., et al. (2010), Concentrations, distribution, and persistence of perfluoroalkylates in sludge-applied soils near Decatur, Alabama, USA, *Environmental Science & Technology*, *44*(22), 8390-8396.

Washington, J. W., et al. (2019), Determining global background soil PFAS loads and the fluorotelomer-based polymer degradation rates that can account for these loads, *Science of the Total Environment*, *651*, 2444-2449.

Weber, A. K., et al. (2017), Geochemical and hydrologic factors controlling subsurface transport of poly- and perfluoroalkyl substances, Cape Cod, Massachusetts, *Environmental Science & Technology*, *51*(8), 4269-4279.

Wei, Z., et al. (2019), Treatment of per- and polyfluoroalkyl substances in landfill leachate: status, chemistry and prospects, *Environmental Science: Water Research & Technology*, *5*, 1814-1835.

Wellington-Laboratories (2021), Wellington Laboratories Catalogue 2016−2018 (https://well-labs.com/wellingtoncatalogue1618.html).

White, S. S., et al. (2011), Gestational and chronic low-dose PFOA exposures and mammary gland growth and differentiation in three generations of CD-1 mice., *Environmental Health Perspectives*, *119*, 1070-1076.

WHO (2017), Some Chemicals Used as Solvents and in Polymer Manufacture, World Health Organization (WHO), International Agency for Research on Cancer (IARC).

Williams, A. J., et al. (2017), The CompTox Chemistry Dashboard: a community data resource for environmental chemistry, *Journal of Cheminformatics*, *9*(1), 1-27.

Xiao, F., et al. (2011), Effects of monovalent cations on the competitive adsorption of perfluoroalkyl acids by kaolinite: Experimental studies and modeling, *Environmental Science & Technology*, *45*(23), 10028–10035.

Xiao, F., et al. (2012), Input characterization of perfluoroalkyl substances in wastewater treatment plants: Source discrimination by exploratory data analysis, *Water Research*, *46*(9), 3101-3109.

Xiao, F., et al. (2015), Perfluorooctane sulfonate (PFOS) and perfluorooctanoate (PFOA) in soils and groundwater of a U.S. metropolitan area: Migration and implications for human exposure, *Water Research*, *72*, 64-74.

Xiao, F. (2017), Emerging poly- and perfluoroalkyl substances in the aquatic environment: A review of current literature, *Water Research*, *124*, 482-495.

Xiao, F., et al. (2017), Identification of novel non-ionic, cationic, zwitterionic, and anionic polyfluoroalkyl substances using UPLC-TOF-MS(E) high-resolution parent ion search, *Analytica Chimica Acta*, *988*, 41-49.

Xiao, F., et al. (2018), PFOA and PFOS are generated from zwitterionic and cationic precursor compounds during water disinfection with chlorine or ozone, *Environmental Science & Technology Letters*, *5*(6), 382-388.

Xiao, F., et al. (2019), Sorption and desorption mechanisms of cationic and zwitterionic per- and polyfluoroalkyl substances in natural soils: Thermodynamics and hysteresis, *Environmental Science & Technology*, *53*(20), 11818-11827.

Xiao, F., et al. (2020), Thermal stability and decomposition of perfluoroalkyl substances on spent granular activated carbon, *Environmental Science & Technology Letters*, *7*, 343-350.

Xiao, F., et al. (2021), Thermal decomposition of anionic, awitterionic, and cationic polyfluoroalkyl substances in aqueous film-forming foams, *Environmental Science & Technology Letters*, *55*, 9885-9894.

Xu, B., et al. (2017), Photocatalytic removal of perfluoroalkyl substances from water and wastewater: Mechanism, kinetics and controlling factors, *Chemosphere*, *189*, 717-729.

Xu, B., et al. (2021), PFAS and their substitutes in groundwater: Occurrence, transformation and remediation, *Journal of Hazardous Materials*, *412*, 125159.

Xu, J., et al. (2020), Enhanced adsorption of perfluorooctanoic acid (PFOA) from water by granular activated carbon supported magnetite nanoparticles, *Science of the Total Environment*, *723*, 137757.

Yan, N., et al. (2020), Transport of GenX in saturated and unsaturated porous media, *Environmental Science & Technology*, *54*(19), 11876-11885.

Yoda, K., et al. (1989), Critical micelle concentrations of fluorocarbon surfactant mixtures in aqueous solution, *Journal of Colloid and Interface Science*, *131*(1), 282-283.

Yong, Z. Y., et al. (2021), The occurrence and distributions of per- and polyfluoroalkyl substances (PFAS) in groundwater after a PFAS leakage incident in 2018, *Environmental Pollution*, *268*, 115395.

Zhao, L., et al. (2014), Comparison of the sorption behaviors and mechanisms of perfluorosulfonates and perfluorocarboxylic acids on three kinds of clay minerals, *Chemosphere*, *114*, 51-58.

Zhao, T., et al. (2010), Molecular dynamics study of alkyl benzene sulfonate at air/water interface: Effect of inorganic salts, *Journal of Physical Chemistry B*, *114*(15), 5025-5033.

Zhou, J., et al. (2021), PFOS dominates PFAS composition in ambient fine particulate matter (PM2.5) collected across North Carolina nearly 20 years after the end of its US production, *Environmetal Science: Processes Impacts*, *23*, 580-587.

Zhou, Z., et al. (2013), Occurrence and transport of perfluoroalkyl acids (PFAAs), including short-chain PFAAs in Tangxun Lake, China, *Environmental Science & Technology*, *47*(16), 9249-9257.

Zhu, B., et al. (2019), Occurrence and degradation potential of fluoroalkylsilane substances as precursors of perfluoroalkyl carboxylic acids, *Environmental Science & Technology*, *53*(9), 4823-4831.